Cross-Hatching Studies—A Critical Review

RUDOLPH J. SWIGART
The Aerospace Corporation, El Segundo, Calif.

I. Introduction

CONSIDERABLE effort has been put forth over the past several years toward identifying the underlying physical mechanisms governing the development of cross-hatched patterns that have been observed to form on the surface of bodies in supersonic and hypersonic flow. These patterns have been noted in a variety of materials under conditions wherein the boundary layer is transitional or turbulent.[1-8] Two such examples are shown in Figs. 1 and 2, taken from Ref. 5. In Fig. 1, patterns are shown etched into a 30° wedge comprised of three different kinds of wood situated behind a sharp steel leading edge. These patterns were formed in a Mach 7.4 flow in the NASA Langley High-Temperature Structures Tunnel. Figure 2 shows a corresponding result on a 36° Teflon cone tested in the same facility at 4° angle of attack.

Practical interest in the cross-hatching phenomenon relates to its effects on heat transfer and body dynamics. With regard to heat transfer, cross-hatching may be considered as a particular form of surface roughness, augmenting the associated smooth-wall heating rate. Evidence of this was observed in the experiments of Lipfert and Genovese.[8] With regard to the effect of cross-hatching on body dynamics, the relationship between surface patterns and roll torques for both sharp-nosed and self-blunting right circular cones has been explored experimentally by several investigators, notably Williams[7] and McDevitt.[9] Williams showed that significant differences in rolling moment

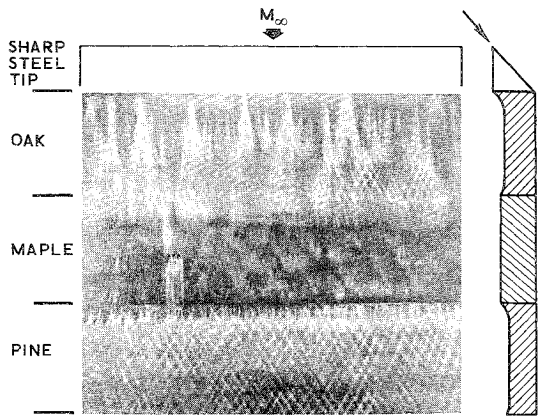

Fig. 1 Cross-hatched patterns in wood.

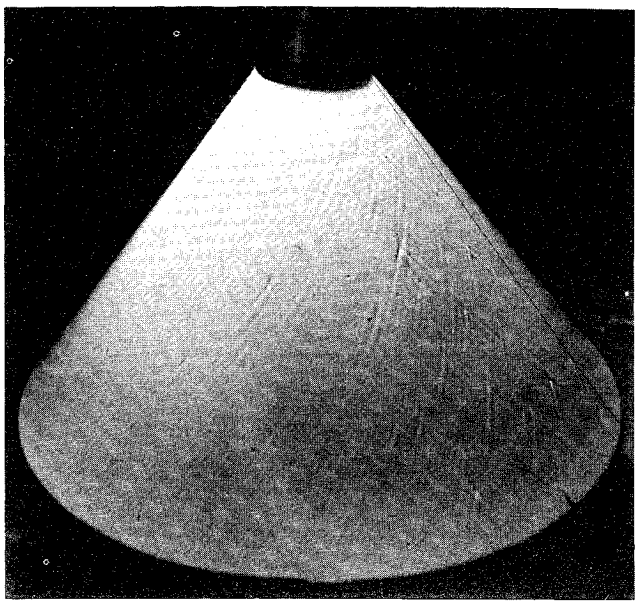

Fig. 2 Cross-hatched patterns in Teflon.

occurred on a 30° Lexan cone when tested under nonablating and ablating conditions. In the ablating condition, a cross-hatched surface pattern developed. Whereas Williams made static measurements using a strain-gage flexural-pivot balance, McDevitt[9] employed a gas-bearing support allowing freedom in roll. Three types of surface patterns were observed during the tests made by McDevitt, namely longitudinal grooves, turbulent wedges, and cross hatching. Correlation of pattern occurrence with observed torques indicated that any of these features can induce roll. Cross hatching had the largest effect, however, inducing substantial rolling moment coefficients due to surface torques. An example of McDevitt's results is shown in Fig. 3, where p is the roll rate. At about 20 sec after model insertion into the tunnel significant cross hatching was observed, corresponding to the beginning of the large subsequent spin-up shown. Note the immediate spin-up in the rerun (shown in the insert), thereby verifying the effect of the pattern on the roll rate.

Concern over the possible deleterious effect of the patterns on heat transfer and body dynamics, and desire to understand

Rudolph Swigart is currently a Staff Engineer in the Fluid Mechanics Department at The Aerospace Corporation. He received a B.S. degree in Aeronautical Engineering from Rensselaer Polytechnic Institute in 1957, an M.S. in the same field from Princeton University in 1958 under support of the Guggenheim Foundation, and a Ph.D. from Stanford University in Aeronautics and Astronautics in 1962. Prior to joining The Aerospace Corporation, Dr. Swigart held positions with Lockheed Missiles and Space Company at their Palo Alto Research Laboratories and Huntsville Research and Engineering Center (1958–1963) and with General Applied Science Laboratories (1963 1966). He has made original contributions in the areas of blast-wave theory, asymmetric hypersonic blunt-body flow theory, asymmetric hypersonic near-wake theory, boundary-layer transition, and sonic-boom alleviation. Dr. Swigart is a member of Sigma Gamma Tau, Tau Beta Pi, and Sigma Xi.

Received December 20, 1973; revision received April 18, 1974.
Index categories: Boundary Layers and Convective Heat Transfer—Turbulent; Supersonic and Hypersonic Flow; Material Ablation.

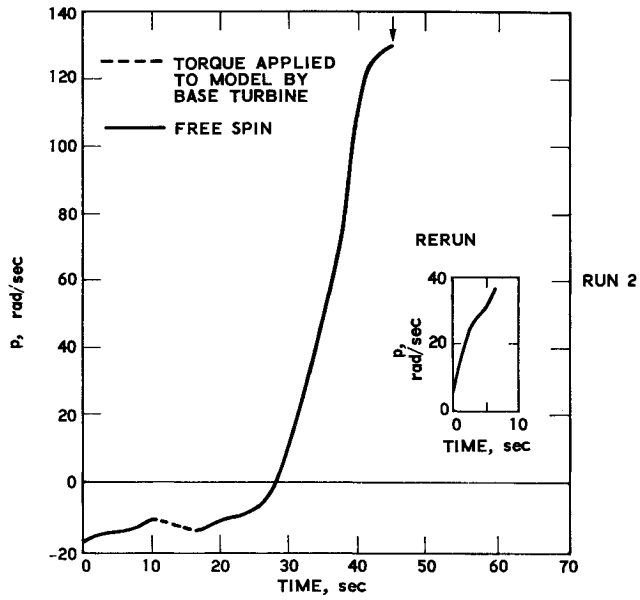

Fig. 3 Roll behavior of ablating 30° NH_4Cl cones at $\alpha = 0°$; from McDevitt.[9]

the cross-hatching phenomenon from a basic standpoint, stimulated a number of theoretical and experimental studies. A review of these studies is given herein. In this review, an effort is made to point out similarities and differences among the approaches taken by various investigators, and to highlight key results. In addition, implications of the studies regarding means of pattern elimination or suppression are discussed.

II. Early Experimental Studies; Phenomenological Mechanisms

A. Canning et al.

Among the earliest work stimulating interest in the cross-hatching phenomenon is that of Canning and his co-workers.[1,2] In these studies, efforts were undertaken to identify conditions of the flow and model geometry under which cross hatching developed. In addition, data correlations were explored and physical models suggested.

Initially, pattern formation was observed in the regions of turbulent flow occurring on Lexan and Delrin cones in the Ames Ballistic Range during a boundary-layer transition study.

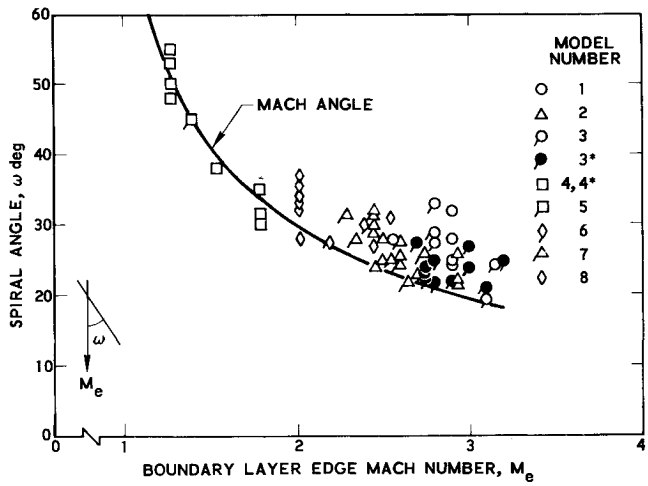

Fig. 4 Spiral pattern angle vs boundary-layer edge Mach number based on data of Canning et al.[4]

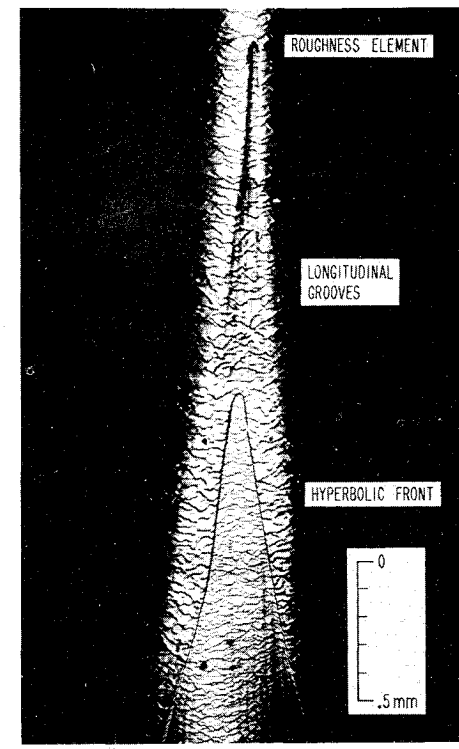

Fig. 5 Turbulent wedge on Lexan model based on data of Canning et al.[4]

Moreover, the occurrence of streamwise grooves provided strong evidence of the presence of longitudinal vortices. These results, coupled with the results of Ref. 3, motivated additional effort in the Ames 3.5-ft hypersonic tunnel to link the observed surface patterns with the aerodynamic and thermodynamic test conditions under which they were produced.[4] Biconic, and concave and convex conical Plexiglas models were tested to obtain large pressure and heating rate changes on a given model, along with large changes in boundary-layer edge Mach number and unit Reynolds number. These tests resulted in numerous examples of cross hatching from which data correlations were developed and a physical model postulated.

One such correlation resulted from the observation that the patterns are due to intersecting grooves that spiral in both directions around the body. A plot of spiral angle (angle between the grooves and the body-generator lines) vs boundary-layer edge Mach number resulted in the correlation shown in Fig. 4. This correlation led to speculation regarding the presence of a standing wave system, and hence the conclusion that cross hatching should not exist in subsonic flow. Two additional correlations based on the work of Canning et al. relate the variation of pattern wave-length to freestream pressure for conical models tested in the ballistic range, and the variation of streamwise pattern spacing to skin friction for test data from both the ballistic range and wind tunnel. All three of these correlations will be discussed further below in light of additional data.

A physical model based on experimental observation such as shown in Fig. 5 was postulated.[4] This model is based on the generation of turbulence wedges that form due to the breakdown of a trailing vortex system generated by a single disturbance source such as a roughness element. It was then postulated that additional longitudinal vortices are generated laterally along the wedge leading edge, which is itself a vortex of roughly hyperbolic shape. The formation of these additional longitudinal vortices results in pressure disturbances that propagate within the Mach cones originating at the points of formation. It is then conjectured that the cross hatched pattern results from the intersection of these Mach cones. Additional experiments per-

formed to investigate the role of disturbance-produced vortices in cross hatch pattern formation are discussed below.

B. Larson and Mateer; Mirels

Additional definitive work directed toward delineating conditions necessary for the formation of cross hatching was performed by Larson and Mateer.[3] Tests carried out in the NASA Ames 3.5-ft Hypersonic Wind Tunnel at Mach 7.4 were designed to study several aspects of the phenomenon, namely to: a) determine whether locally supersonic flow is a necessary condition for pattern formation; b) study the effects of tip geometry; c) determine if cross hatching occurs on two-dimensional as well as conical models; d) obtain quantitative information regarding patterns angles, spacing, and depth; and e) determine the dependency of the pattern on time and amount of surface removal.

The local supersonic flow requirement was investigated by testing steel-tipped Lucite cones of different cone angle such that boundary-layer edge Mach numbers, M_e, both above and below unity were obtained. Typical results are shown in Figs. 6 and 7. Figure 6a shows a 50° half-angle cone ($M_e = 1.3$) on which cross hatching is clearly evident. For the 55° half-angle cone ($M_e = 0.9$), no cross hatching was observed, however (Fig. 6b). A striking result in which both supersonic and subsonic rays were achieved during the same test is shown in Fig. 7 wherein a 55° half-angle cone was tested at 5° angle of attack; hence, the windward rays are subsonic and the leeward mostly all supersonic. Cross hatching is observed on the upper (leeward) portion of the cone, but not on the lower (windward) portion. Thus, the requirement of locally supersonic flow for pattern occurrence is clearly demonstrated.

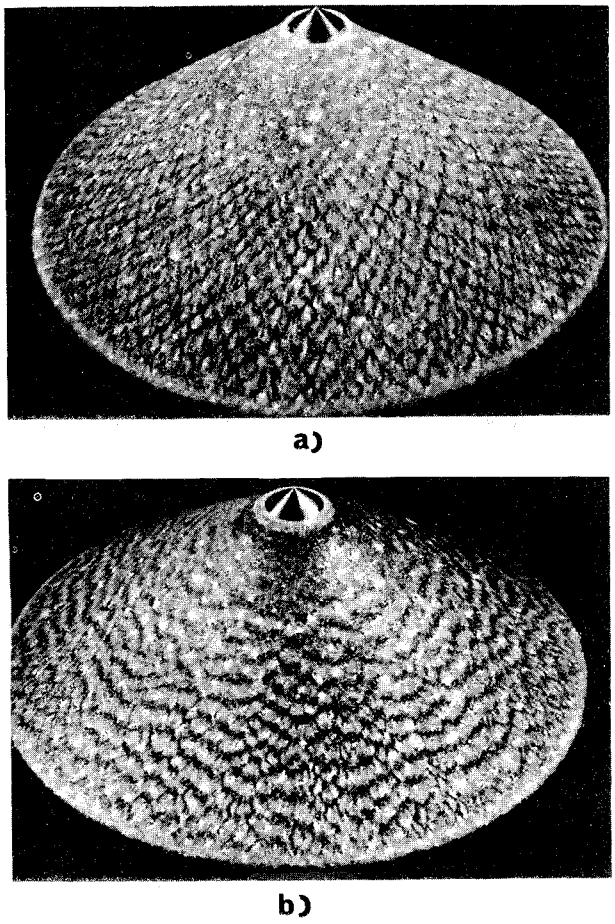

Fig. 6 a) 50° half-angle Lucite cone, surface Mach number = 1.3; from Larson and Mateer.[3] b) 55° half-angle Lucite cone, surface Mach number = 0.9; from Larson and Mateer.[3]

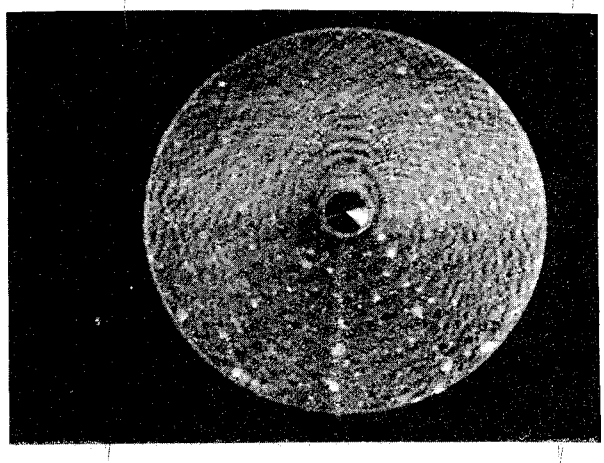

Fig. 7 Lucite 55° half-angle cone tested at 5° angle of attack, lower is windward; from Larson and Mateer.[3]

To examine the effects of tip blunting, both steel-tipped and self-blunting 50° half-angle cones were tested. Cross hatching was observed on both models, the position of boundary-layer transition being dominated by surface roughness generated during the ablation process.

To answer the question of whether cross hatching would form on two-dimensional as well as axisymmetric models, a 35° Lucite wedge with steel leading edge was tested. Cross hatching was observed, thereby demonstrating its occurrence in two-dimensional as well as axisymmetric flows.

The same correlation of cross hatch pattern angle with boundary-layer edge Mach number as quoted by Canning (Fig. 4) was noted by Larson and Mateer in their tests. Groove spacing, however, varied by as much as a factor of two in random manner on a given model and no correlation of this quantity was attempted. In general, groove depth was measured to be approximately 10% of the mean surface ablation depth.

Observations of the dependence of the pattern on time yielded interesting results. In one particular test involving a 50° Lexan cone, patterns were observed to form, disappear, and be replaced by patterns of a larger wavelength. Moreover, pattern depth increased with time, late-time patterns resembling the so-called regmaglypt patterns frequently observed on meteorites.[3]

Larson and Mateer further observed that the presence of supersonic flow and a turbulent boundary layer were necessary but not sufficient conditions for cross hatching to occur, since results for a 5° cone indicated absence of the pattern. Moreover, shadowgraphs of the 5° cone and of a 30° cone that exhibited cross hatching showed clear indications of shock waves in the shock layer of the 30° cone, but indicated the shock layer of the 5° cone to be relatively free of shock waves. Hence, it was postulated that a third requirement for the occurrence of cross hatching is the presence of a boundary layer sufficiently thin such that the surface pressure distribution is essentially that of the supersonic portion of the layer. This led to a suggested mechanism whereby disturbance-generated shock waves cause differential ablation of the surface to generate the pattern.

A similar mechanism was proposed by Mirels[10] based on a groove marching process. In this process, a small roughness element would cause a weak, essentially conical, shock to form. This shock intersects the body surface and local overpressures at the base of the waves cause increased ablation, resulting in grooves. Nonlinear interaction between the initially weak wave and the ablative surface would result in increased local wave strength, thereby increasing the groove ablation rate. Because of the enhanced ablation, the local inviscid flow is equivalent to low supersonic Mach-number flow over a two-dimensional body. The trailing shock associated with this flow would intersect the ablative surface, causing the process to repeat itself (Fig. 8).

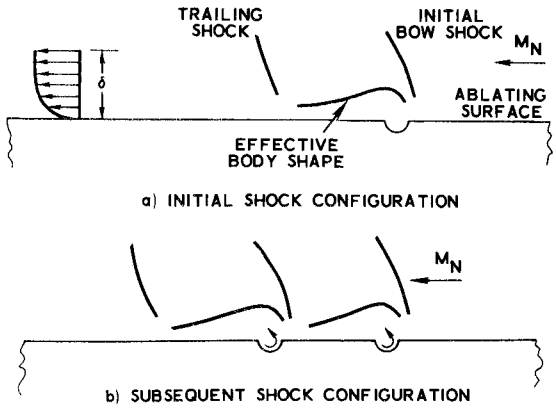

Fig. 8 Representation of marching process showing flow normal to initial shock; from Mirels.[10]

It is postulated that each of numerous surface roughness elements starts separate systems of waves that intersect to form the pattern.

This mechanism was investigated by Laganelli and Zempel[6] (discussed below) and not borne out, however. Thus the shock waves observed by Larson and Mateer are apparently a result, rather than a cause, of the pattern.

C. Laganelli and Nestler; Laganelli and Zempel

Additional investigation of cross hatching pattern characteristics and conditions for occurrence was carried out by Laganelli and Nestler[5] and Laganelli and Zempel.[6] Laganelli and Nestler considered char-forming materials (carbon phenolic, phenolic nylon, and wood), a subliming ablator (epoxy resin) and two melting ablators (Teflon and Lexan). The carbon phenolic, phenolic nylon, and epoxy resin models were tested in the Malta rocket exhaust facility, whereas, wood, Lexan, and Teflon models were tested in the NASA Langley 8-ft Structures Tunnel, and a Teflon model was tested in the Cornell Aeronautical Lab. Facility. Phenolic-nylon afterbodies tested in the Malta facility exhibited cross hatching similar to what had been observed on other tests previously discussed. When a carbon phenolic sphere-cone tip was tested with a phenolic-nylon afterbody, however, cross hatching was observed on the afterbody only. Possible explanations for this are that the flow was laminar over the nose tip or that, since the models were self-illuminating, the patterns existed but could not be observed. In one of the tests conducted in the Malta facility, a model was rotated at 2000 rpm. The pattern half-angle relative to a given meridian was noted to shift in a direction consistent with the local cross flow.

Among the most interesting results with a char-forming material were those obtained from steel-tipped wood wedges and cones tested in the Langley Structures Tunnel (the wedge is shown in Fig. 1). In Fig. 1, note that patterns formed within the turbulence wedges on the oak section, but not outside, indicating that transitional/turbulent flow is necessary for the patterns to develop. Note further that the patterns do not persist through the maple section of the model, possibly because of insufficient ablation. Moreover, the pattern development in the pine occurs without the presence of turbulence wedges, since the flow is already turbulent there. It is suggested by Laganelli and Nestler that this latter observation appears to negate the mechanism postulated by Canning (discussed previously) that turbulence wedges are necessary for the initiation and propagation of cross hatched patterns. It is not considered to be inconsistent by this writer, however, since the turbulence wedges appear to cover the entire lateral extent of the model by the end of the oak section.

An additional observation from the work of Laganelli and Nestler is the occurrence of what might be termed positive and negative patterns on melting/subliming materials and charring materials, respectively (Fig. 9). The patterns on the melting or subliming materials are characterized by right- and left-running grooves delineating a raised island between, whereas charring materials are characterized by narrow ridges bounding a recessed island. A possible explanation for this has been advanced by Persen,[11] who studied the cross hatching phenomena using the hydraulic analogy. The equation for the liquid-layer depth is simply Bernoulli's equation which, if the local depth is interpreted as the enthalpy, is equivalent to the energy equation for a high-speed gas layer next to the surface. The surface height perturbation is consequently equivalent to an enthalpy perturbation which, if positive, would mean a raised part of the surface if the surface melts, but implies a burned-out valley when the surface chars. This is consistent with the observed results of Laganelli and Nestler.

Laganelli and Zempel[6] investigated the effects of surface disturbances on the cross hatched pattern. They tested 36° half-angle sharp-tipped Teflon cones (an example is shown in Fig. 2) in the NASA Langley 8-ft High-Temperature Structures Tunnel and investigated, among other things, the effect of single and multiple rows and columns of drilled holes and pins at various longitudinal and lateral spacings and depths. The results clearly indicated that the disturbances only affected the pattern locally, and did not govern over-all pattern development. Thus, the postulated disturbance-generated shock-wave mechanisms of Larson and Mateer and Mirels previously discussed do not appear to cause pattern formation.

D. Williams

Williams[7] obtained cross hatched patterns on a number of sharp-nosed cones tested at a freestream Mach number of 6. Patterns were obtained in camphor, Korotherm, and naphthalene over a range of cone angles and surface pressures. Under the conditions of the tests, camphor and Korotherm ablate by

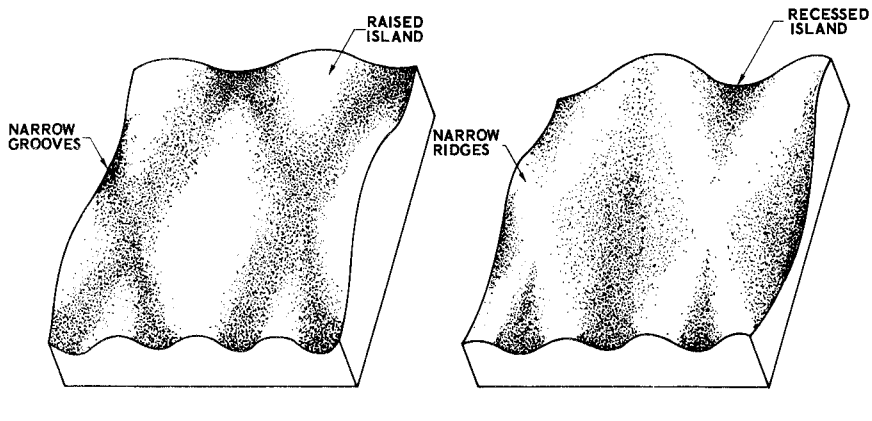

Fig. 9 Typical characteristics of diamond-shaped ablation patterns; from Laganelli and Nestler.

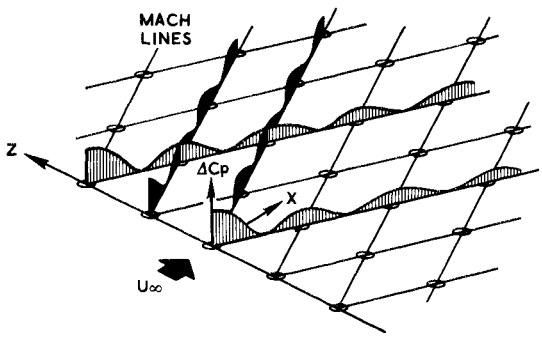

Fig. 10 Perturbation pressure distribution resulting from analysis of Tobak.[12]

sublimation, whereas naphthalene passes through the liquid state and vaporizes. Based on the test data, the previously noted correlation between pattern wavelength and surface pressure suggested by Canning et al.[1] was obtained for the camphor models. This correlation will be discussed further below.

The abovementioned background of experimental evidence and postulated mechanisms further stimulated a number of detailed theoretical studies and related experiments. These are discussed in the following section.

III. Theoretical Studies and Related Experiments

A. Vortex Mechanisms

Experimental evidence of the presence of streamwise vortices, both upstream and in the neighborhood of cross hatched surface patterns, engendered a number of theoretical and experimental studies to investigate the possible relationship between cross hatching and vortices. A phenomenological model postulated by Canning has been previously discussed. Other studies of note are those of Tobak,[12] Persen,[11,13] and Stock and Ginoux.[14]

Tobak, utilizing the results of linearized wing theory, showed how spanwise periodically varying downwash, generated by uniformly spaced counter-rotating longitudinal vortices, induces a periodically varying pressure perturbation both spanwise and longitudinally. The result is a peaking of the perturbation pressure field at the intersections of Mach lines as shown in Fig. 10. It is conjectured that such a pressure distribution would result in a surface pattern consistent with observations. The question of the origin of longitudinal vortices is discussed at length in Ref. 12.

Persen[11,13] investigated the relationship between streamwise directed vortices and cross hatching both experimentally and analytically. Based on evidence of the concurrent presence of streamwise striations and cross hatching noted by Canning, Laganelli and Nestler, and others, he studied the possible relationship and interaction between these two types of surface patterns.[13] By means of the hydraulic analogy, he related the flow of water over a thin paint coat of spanwise varying depth to supersonic flow over a surface with streamwise directed vortices. Cross hatched patterns superposed over longitudinal striations were observed, analogous to patterns that had been observed both in ground tests and on recovered flight vehicles.

Stock and Ginoux[14] investigated the possible role of streamwise vortices in the initiation of cross hatching by introducing vortices of different intensities into the boundary layer and observing the effect, if any, on the subsequent cross-hatched pattern. This was done by using three-dimensional roughness elements of different height, diameter, and spacing, and by the use of backward-facing steps of different heights. The results show that, although both the roughness element and step heights were varied over a substantial range, the patterns remain essentially unchanged. Hence, Stock and Ginoux concluded that streamwise vortices are not necessary for cross hatching to occur.

Hence, as far as the possible relationship between streamwise vortices and cross hatching is concerned, based on the work of Stock and Ginoux it may be concluded that streamwise vortices are not necessary for cross hatching to occur.

B. Differential Ablation Mechanism

Based on the occurrence of patterns in subliming materials, a number of studies investigating development of patterns by differential ablation have been carried out.

As indicated previously, for a gaseous outer flow cross-hatched surface patterns have been observed to occur only under conditions wherein the boundary-layer flow is turbulent and the outer-edge Mach number supersonic. Hence, the general framework of the approaches of several investigators is linearized analysis of supersonic turbulent boundary-layer flow perturbed by a wave-shaped wall, the linearized approach considered valid for early stages of pattern development.

Both steady and unsteady approaches have been taken, the objective of the steady approaches being to determine if relative phasing of surface pressure, shear, and heat transfer with the wavy wall conducive to pattern growth could be obtained.

1) *Inger*

Inger[15-19] considered a number of steady-state analytical models ranging in complexity from simple representation of the boundary-layer flow and wall boundary conditions to complex models considering a viscous sublayer and mass addition. In his most comprehensive analysis,[17-19] he considered the boundary layer to be comprised of an inviscid outer flow and a viscous sublayer. Only two-dimensional flow past a wavy wall is considered, the two-dimensional assumption being valid since, for moderate supersonic speeds, the problem can always be broken down into component problems for the flow normal and parallel to the waves.[18] The inviscid portion of the boundary-layer flow is solved numerically, the governing equation being the so-called Lighthill's equation for the perturbation pressure,[20,21] and an analytical solution is obtained in the viscous sublayer. Results for relative phasing of pressure, shear, and heat-transfer perturbations for the cases of high and low mean heat-transfer rates in the limiting cases of the boundary-layer thickness large and small compared with wall wavelength are shown in Fig. 11. In Fig. 11, $\dot{q}_{w_o}$ is the mean wall heat-transfer rate, p', $\dot{q}_w'$, τ' are the pressure, heat-transfer, and shear perturbations at the wall, respectively, and $\alpha\delta_o = 2\pi\delta_o/\lambda$ is the unperturbed boundary-layer thickness to wall wavelength ratio. Note that, for nondimensionalized wave number $\alpha\delta_o$ small and a

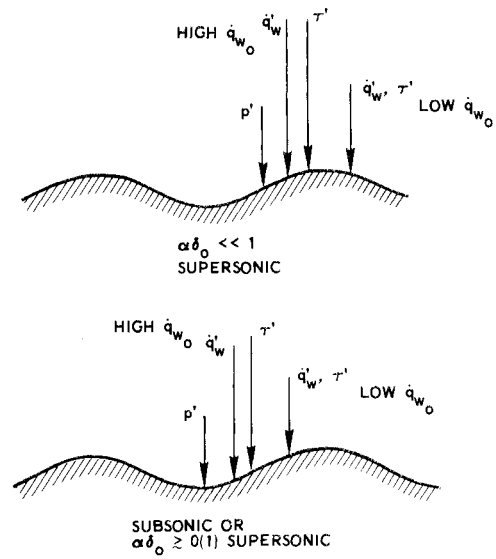

Fig. 11 Phase relations of wall perturbation maxima for high and low mean heat transfer rate; based on analysis of Inger.[17-19]

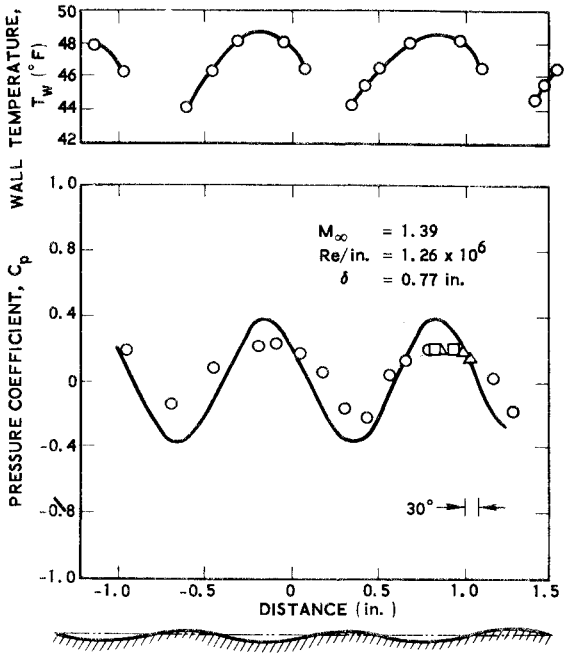

Fig. 12 Comparison of theory of Inger with experiment for pressure and surface temperature on a wavy wall.

supersonic outer flow, the surface pressure peaks at the maximum slope point of the wall, whereas for subsonic outer flow or supersonic outer flow with $\alpha\delta_o$ large, the surface pressure peaks in the wave trough. Thus, the wall phasing for the solution with a subsonic outer-edge Mach number is the same as for the large $\alpha\delta_o$, supersonic Mach number case. This is as might be expected, however, since under those conditions the pattern is buried deep in the subsonic portion of the boundary layer. On the other hand, for small $\alpha\delta_o$ the boundary layer follows the wall and the solution tends toward the uniform supersonic flow results, as also might be anticipated. Moreover, note that the analytical sublayer solution results in the surface shear and heat transfer lagging the pressure by 120° for the case of low surface heat transfer, and by 60° and 42°, respectively, for the case of high surface heat transfer. Additionally, for the case of the wall slightly warmer than the freestream flow, the sublayer solution indicates that the wall temperature leads the pressure by 30°.

Results of Inger's theory were compared with surface pressure and temperature distributions obtained by Williams and Inger[16,17] from tests of high subsonic and low supersonic flows past a nonablating two-dimensional wavy wall. The wall had a wavelength of 1 in., an amplitude of 0.03 in., and was

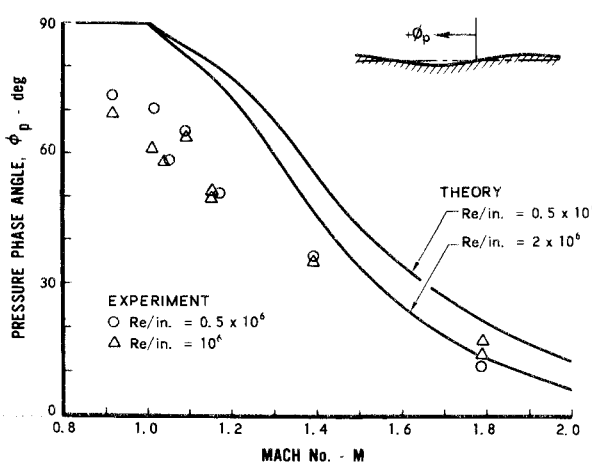

Fig. 13 Comparison of theoretical and experimental pressure phase shifts based on results of Inger.[17-19]

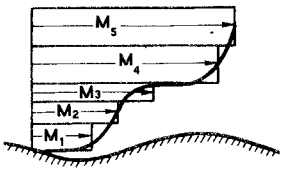

Fig. 14 Generalized layered approximation of Conrad and Donaldson.

instrumented with surface-pressure orifices. In addition, in an effort to measure the surface temperature distribution the surface of the wall was coated with temperature-sensitive paint. Results for a freestream Mach number of 1.39, a freestream Reynolds number of 1.26-million/in., and a turbulent boundary-layer thickness of 0.77 in. are shown in Fig. 12 and compared with Inger's theory. Pressure phasing is predicted within about 30°, whereas pressure coefficient amplitude is off as much as 50–60% at the maximum and minimum points. Note that the temperature distribution is accurately predicted and is peaking in the wall troughs. The experimental temperature and pressure distributions appear to be peaking at about the same place, however. Therefore, the theoretically predicted 30° lead of temperature over pressure is not borne out by the data shown in Fig. 12. Results for the pressure phasing from all the tests are summarized and compared with theory in Fig. 13. Substantial phase shifts are noted at the lower Mach numbers, differences between theory and experiment being attributable, at least in part, to inaccuracy of the linear theory in the trasonic regime.

Thus, it may be concluded that the analysis of Inger accurately predicts the temperature distribution over a wavy wall, but is only fairly accurate in predicting the pressure distribution at transonic Mach numbers. Since only the two-dimensional problem is being considered, it is precisely the transonic Mach numbers that are of interest due to the fact that the component of boundary-layer edge Mach number normal to the waves (edge Mach number for the two-dimensional problem) is close to sonic since the spiral angle ω has been observed to be at the Mach angle or slightly above (Fig. 4).

2) *Conrad, Donaldson, and Snedeker*

Another steady-state analysis to the cross-hatching problem worthy of note is that of Conrad, Donaldson, and Snedeker[22] in which the full three-dimensional problem was treated, i.e., the flow was not decomposed into components normal and parallel to the wave and the normal problem treated as previously discussed. The boundary layer Mach-number profile was broken down into a number of layers of constant Mach-number flow in each layer (Fig. 14) and the problem formulated in terms of a

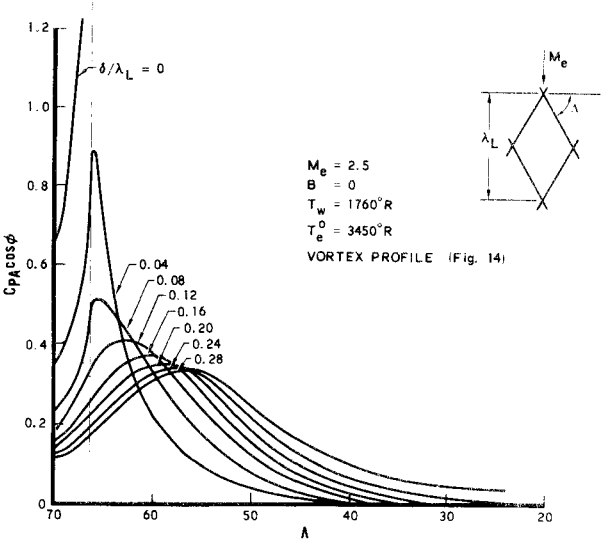

Fig. 15 Results of layered analysis—Teflon cone, vortex profile; based on analysis of Conrad, Donaldson, and Snedeker.[22]

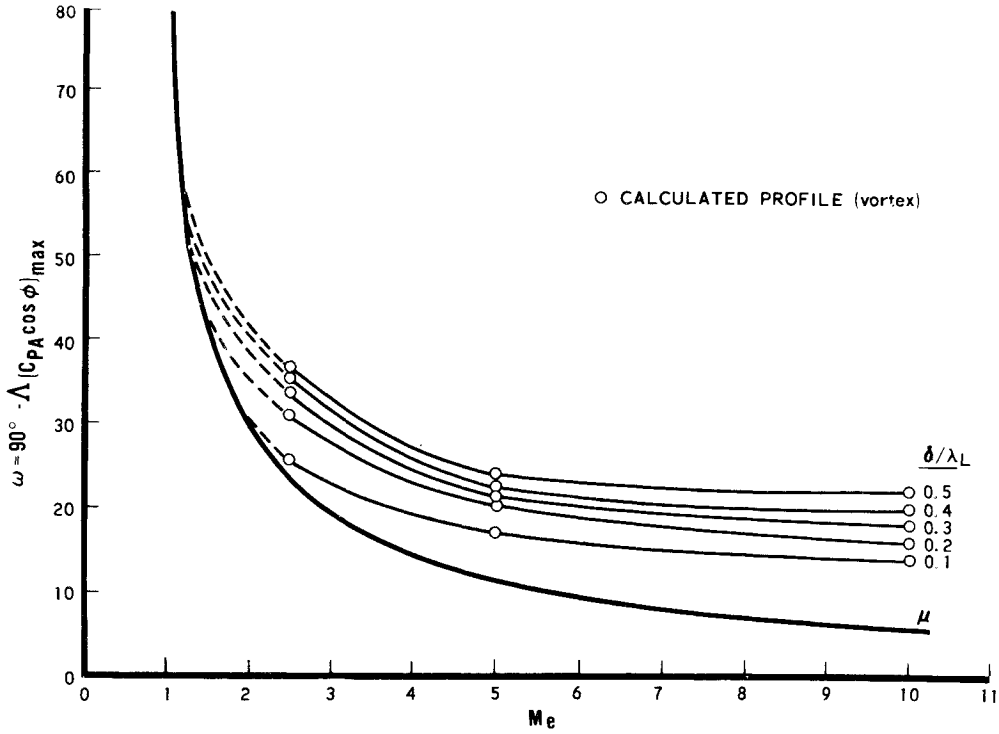

Fig. 16 Results of layered analysis—pattern angle vs edge Mach number; based on analysis of Conrad, Donaldson, and Snedeker.[22]

perturbation velocity potential which, in each layer, satisfies either the three-dimensional wave equation or LaPlace's equation depending on whether the Mach number in the layer is supersonic or subsonic, respectively.

Conrad, Donaldson, and Snedeker assumed, however, that heat-transfer rate is proportional to pressure, an assumption that, based on the results of Inger (Fig. 11) is fairly accurate when the heat-transfer rate is high, a condition that prevails for an ablating wall. Under this assumption, the analysis indicates that those wavelengths for which $(\delta/\lambda_L)C_{p_A}\cos\phi$ is a maximum will have the greatest rate of amplification (δ is the boundary-layer thickness, λ_L the longitudinal wavelength, C_{p_A} the pressure-coefficient amplitude, and ϕ the phase angle between the pressure and the wall). To determine the pattern angle $\omega = \pi/2 - \Lambda$ (Λ is the sweep angle) for which this occurs, solutions were obtained over a range of angles for given values of δ/λ_L. The results for the flow over the Teflon cone shown in Fig. 2 are given in Fig. 15. The conditions for the calculations are shown in the figure, M_e being the boundary-layer edge Mach number, B the wall blowing parameter, T_w the wall temperature, and T_e^o the edge total temperature. The dashed vertical line represents the Mach angle. The results shown were obtained using a boundary-layer Mach number profile characteristic of a flow containing longitudinal vortices. These profiles are characterized by a plateau region as shown in Fig. 14, being similar to the previously discussed two-step profiles investigated by Inger. Maxima are noted for all values of δ/λ_L, being sharper at the smaller values. When calculations were carried out using conventional profiles, no clearly definable maxima were obtained, either with or without wall blowing. Results similar to those obtained using the vortex profiles were achieved using conventional profiles when a substantial reduction in wall temperature was made, however. Corresponding calculations were carried out at edge Mach numbers of 5 and 10 and the results using the vortex profiles are summarized in Fig. 16, where the wave angle corresponding to peak amplification is plotted as a function of edge Mach number. These results indicate that the wave angle will be close to the Mach angle for small values of the ratio δ/λ_L, but above it for larger values of δ/λ_L, the difference increasing as M_e increases. This result is consistent with the data of Fig. 4.

In addition, these results were utilized by White and Grabow[23,24] for defining the outer (inviscid) flow in combination with various inner (viscous) flow and surface response models. The results of the various composite theories were compared with data for Teflon and other materials as shown in Figs. 17a and b. For the composite surface-flow theory, the heat transfer is in phase with the surface pressure, and the inviscid solution determines the wave angle dependence on the wavelength parameter directly. Good agreement with the data for this theory is shown. These results are discussed in further detail in Sec. V.

Thus, the analysis of Conrad, Donaldson, and Snedeker appears useful for predicting a preferred wave angle. Moreover, the analysis predicts a dependence of wave angle on the

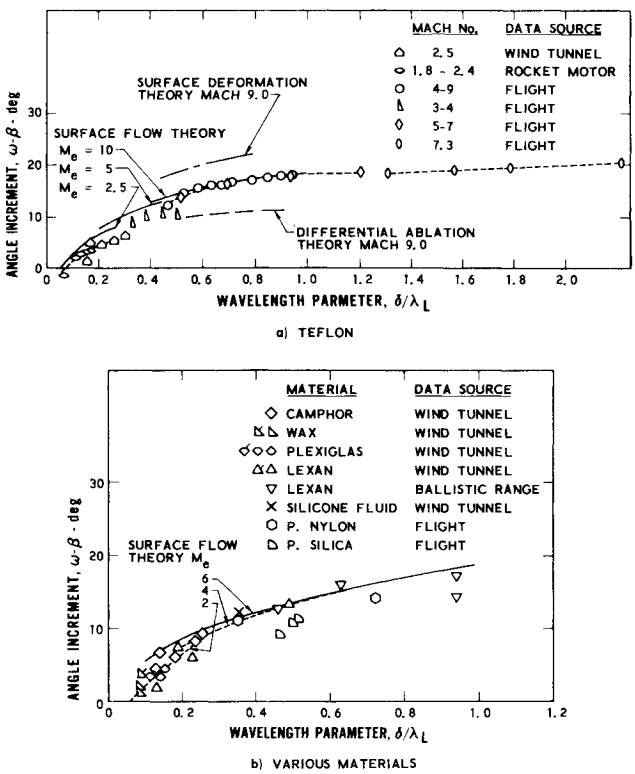

Fig. 17 Wave-angle correlation developed by White and Grabow.[23,24]

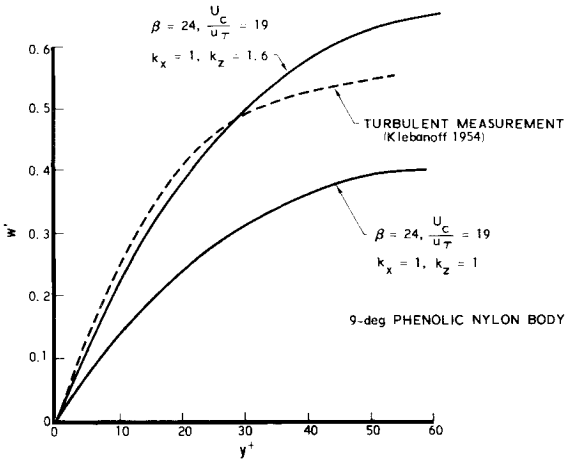

Fig. 18 Distribution of rms spanwise velocity fluctuations near the wall as determined by Lew and Li.[25]

ratio of boundary-layer thickness to longitudinal wavelength that has been shown to compare well with data.

3) *Unsteady Approaches*

Unsteady approaches to the subliming ablator problem were taken by Lew and Li,[25] Lees and Kubota,[26] and Lane and Ruger (unpublished). The basic idea in the unsteady approaches is that, analogous to laminar stability theory, the mean turbulent flow is assumed to be influenced by a disturbance (the wavy wall) that is expandable in Fourier series. Each Fourier component of the wall is given by

$$h = \varepsilon e^{i(\alpha x + \beta z - \omega t)} \tag{1}$$

where x and z are Cartesian coordinates in the plane of the undisturbed surface, ε is the surface amplitude, α, β are the wave numbers in the x, z directions, respectively, and the quantity ω is complex. Introducing the ratio

$$c = \omega/\alpha = c_r + ic_i \tag{2}$$

c_r denotes the velocity of propagation of the wave in the x-direction (phase velocity) and c_i determines the degree of amplification or damping of the wave (depending on whether it is positive or negative). In most all of the analyses undertaken pertaining to the cross-hatching problem, perturbations of the mean turbulent flow due to turbulent fluctuations are neglected compared with perturbations due to the wavy wall. Hence, the flow variables are expanded in terms of mean and perturbation quantities, where the perturbation quantities are assumed to have Fourier components corresponding to those of the wall. For example, the velocity in the x-direction is assumed to have an expansion of the form

$$u(x, y, z, t) = u(y) + u'(y)e^{i(\alpha x + \beta z - \omega t)} \tag{3}$$

where $u'(y)$ is complex, thereby having an amplitude and phase relative to the wall as a function of y. Substitution of these expansions into the governing equations and elimination of mean flow quantities results in governing equations for the perturbation quantities involving α, β, and ω. For given assumed values of α and β, the complex eigenvalue ω is obtained. Those values of α and β for which the imaginary part of ω takes on its maximum value will have the largest growth rate, therefore dominating the pattern. It is these dominant wavelengths that are sought.

A unique approach to the viscous unsteady problem was taken by Lew and Li[25] in which a viscous sublayer beneath an assumed inviscid outer portion of the boundary layer was again considered. However, based on ideas developed by Sternberg[27,28] and Schubert and Corcos[29] that the sublayer is driven by fluctuating quantities at its outer edge, Lew and Li considered the problem of a sublayer driven by an outer inviscid flow that is perturbed by a three-dimensional wavy wall. Solutions for the turbulent velocity flowfield in the sublayer were calculated for choices of lateral and longitudinal wave number and compared with experimental measurements. A typical result is shown in Fig. 18. The distribution through the sublayer of the lateral rms fluctuating velocity component w' for longitudinal and lateral wave numbers (in their notation) k_x, k_z of (1.0, 1.6) and (1.0, 1.0) is compared with experimental results of Klebanoff[30] (β is a parameter occurring in the description of the mean velocity profile, U_c is the phase velocity, and u_τ the friction velocity). Relatively poor agreement is obtained for the (1.0, 1.0) case. The results for the (1.0, 1.6) case show substantially better agreement with experiment, however, indicating the pattern wavelengths and wave angles most likely to occur.

Two separate investigations of the subliming ablator problem were carried out by Lees and Kubota.[26] In the first, stability was investigated by means of an unsteady approach embodying a viscous sublayer. By coupling an integral solution for the sublayer with a numerical solution to Lighthill's equation for the assumed inviscid outer portion of the boundary layer, the heat-transfer fluctuations were obtained in terms of the wall wave number, the thermal diffusivity, and the complex wave speed. When the thermal diffusivity is taken as zero (insulated wall), the solution for all wave numbers is unstable and no preferred wavelength and wave angle are indicated. However, when finite material conductivity is introduced, wave numbers and wave angles of peak instability are indicated (Fig. 19). In Fig. 19, θ is the wave angle, $\alpha = 2\pi\delta/\lambda$ the nondimensional longitudinal wave number (λ is the wavelength), c_i the amplification factor, $K_s/v_s\delta$ the diffusivity parameter, K_s being the thermal diffusivity of the surface, v_s the mean surface ablation rate, and δ the boundary-layer thickness. For $M_\infty = 2.6$, the Mach angle μ is 22.6°. Note that peak instability is indicated for θ between 25° and 35°. This is slightly larger than the Mach angle, again consistent with the data of Fig. 4.

A numerical solution to the complete unsteady viscous problem of supersonic turbulent boundary-layer flow over a wavy wall with coupled surface boundary conditions has also been obtained for the subliming ablator by Lees and Kubota.[26] The object of this formulation is to treat the more exact problem by removing some of the assumptions of the earlier analysis previously described. A result for ablating Teflon, treated as a sublimer, was obtained, again for a boundary-layer edge Mach number of 2.6. Regions of peak instability in wave number-wave angle space were obtained, indicating that a preferred pattern geometry would develop with a preferred wave angle between 33° and 38°.

Lane and Ruger (unpublished) also treated the full unsteady problem in which viscosity is considered throughout the turbulent boundary layer and appropriate mass and energy balances are considered at the wall boundary. Contrary to the results of Lees and Kubota previously discussed, however, Lane

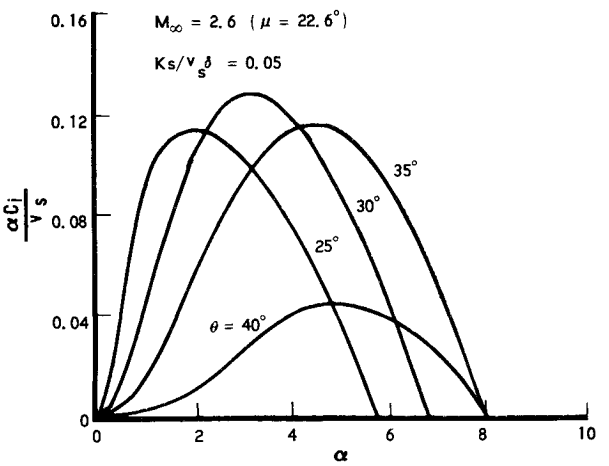

Fig. 19 Results of analysis of Lees and Kubota[26] considering finite thermal conductivity.

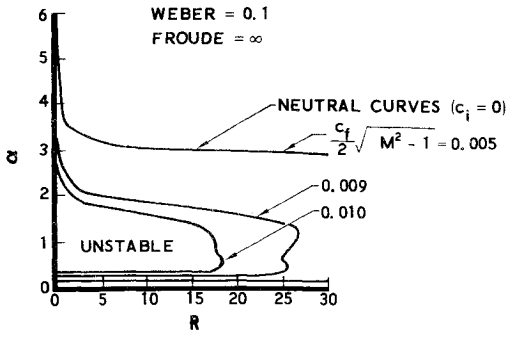

Fig. 20 Neutral stability contours based on analysis of Nachtsheim.[31]

and Ruger found no regions of instability at wavelengths of practical interest for three different materials (Teflon, camphor, and ammonium chloride) at conditions corresponding to experiment.

Thus, based on the work of Inger, Conrad et al., Lew and Li, and Lees and Kubota, coupled conditions between the boundary-layer flow and a subliming ablator conducive to the development of a cross-hatched surface pattern are physically realizable. The analysis of Lane and Ruger, on the other hand, does not predict pattern development for the sublimer. Hence, further work is needed before a definite conclusion can be drawn regarding a firm theoretical basis for differential ablation as a mechanism for the development of cross-hatched surface patterns.

C. Liquid Layer Mechanism

Several investigators, notably Nachtsheim,[31] Ko,[26] and Nayfeh and Saric[32] investigated the stability of a thin liquid layer as a possible mechanism for the development of cross-hatched surface patterns.

Nachtsheim[31] investigated the case of a viscous layer driven by a uniform inviscid outer flow of velocity different from the mean surface velocity of the liquid. The outer-flow properties enter the problem through the so-called interaction parameter $c_f/2(M^2-1)^{1/2}$, where c_f is the skin-friction coefficient at the gas-liquid interface based on the liquid surface shear but normalized with respect to the gas-flow dynamic pressure, and M is the outer-flow Mach number normal to the wave fronts. Numerical solutions to the eigenvalue problem were obtained, and typical results are shown in Fig. 20 where curves of neutral stability ($c_i = 0$) are shown as functions of the interaction parameter for fixed values of the Weber and Froude numbers (α is the wave number and R_L the liquid-layer Reynolds number).

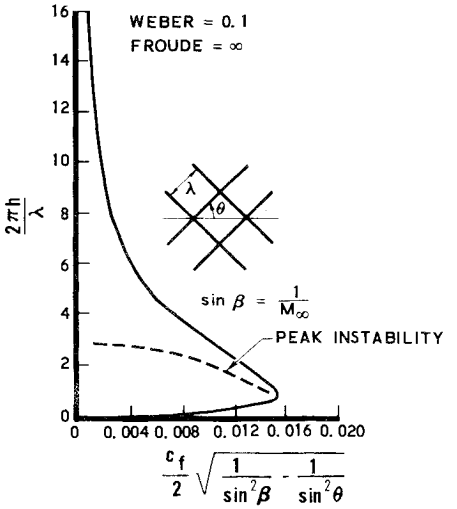

Fig. 21 Solution in neighborhood of $R = 0$ based on analysis of Nachtsheim.[31]

The Weber and Froude numbers are essentially the ratios of inertial forces to surface-tension and gravity forces, respectively. Thus, for a given value of interaction parameter, a cutoff value of liquid-layer Reynolds number is indicated above which no patterns should form. In addition, when αc_i is plotted vs R_L, it appears that $R_L = 0$ is a point of neutral stability for all wave numbers. To investigate this further, Nachtsheim developed analytical solutions in the neighborhood of $R_L = 0$, the results being shown in Fig. 21. The abscissa is simply the interaction parameter written in terms of freestream quantities and the wave angle. Thus, for a given value of interaction parameter below the cutoff value, both a preferred wave angle and wave length are indicated. It is interesting to note that, in the absence of surface tension ($W = \infty$), neutral stability cannot be obtained from Nachtsheim's analysis; all solutions are unstable. Thus, finite surface tension is essential to obtaining a preferred pattern from his theory.

A similar analysis of the liquid-layer stability was carried out by Ko.[26] However, in place of a uniform external flow Ko assumed a representative turbulent-flow power-law profile. Neglecting viscosity in the external flow, he numerically integrated the governing equation for the perturbation pressure through the outer layer to obtain the outer-edge boundary conditions for the liquid-layer stability problem. In addition, the gravitational body force was neglected. Results similar to Nachtsheim's were obtained, with both a preferred wave angle and wave length predicted. However, since no results were presented for the same values of the parameters used by Nachtsheim, a direct comparison to ascertain the effect of the outer-flow differences could not be made.

A perturbation solution for small αR_L and generally-directed body forces was developed by Nayfeh and Saric[32] and analytic solutions obtained. Results of a two- and four-term expansion are compared with the numerical results of Nachtsheim in Fig. 22. Shown there are calculations of growth rate as a function of wave number at two values of liquid-layer Reynolds number and other conditions constant at the indicated values. Note that, whereas both expansions predict the lower cutoff wave number, neither accurately predicts the maximum growth rate and corresponding wave number, or the second cutoff wave number. Thus, the accuracy of the analytical solutions is restricted to the

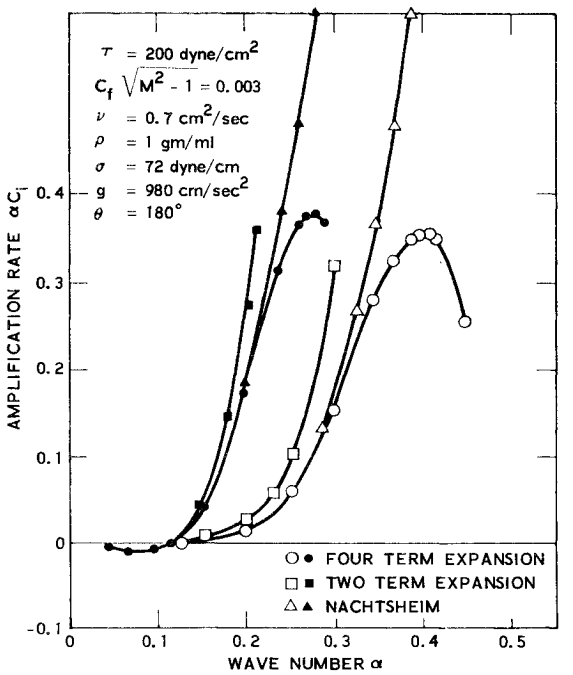

Fig. 22 Amplification rate vs wave number for three solution techniques; from Nayfeh and Saric.[33] Solid symbols are for $R_L = 1.0$, blank symbols for $R_L = 0.1$.

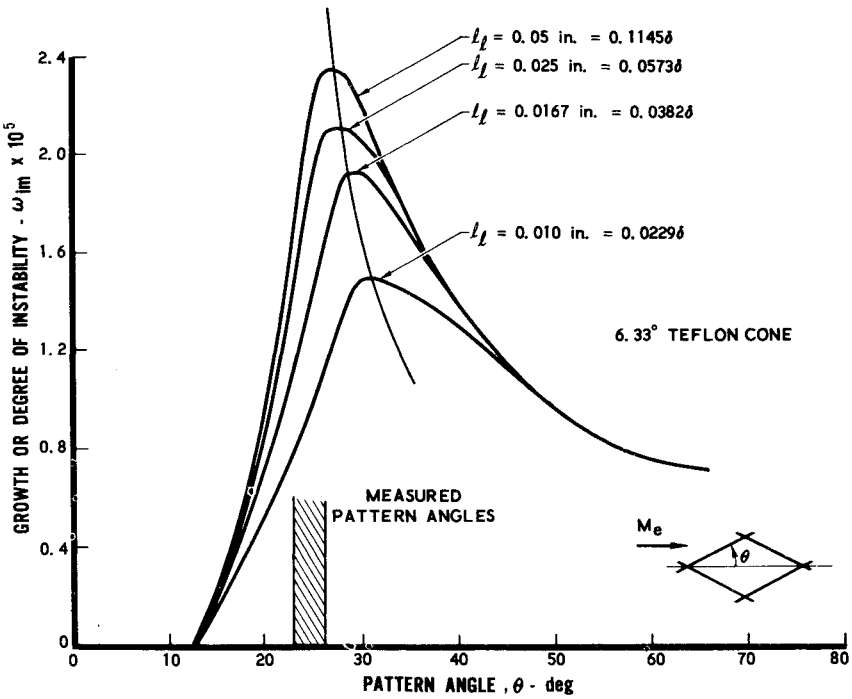

Fig. 23 Instability parameter vs pattern angle based on analysis of Lane and compared with data.

range imposed by the assumptions in their derivation, namely αR_L small.

An interesting comment on Nachtsheim's work is put forth by Craik[33] in which he shows that the instabilities discussed by Nachtsheim are directly related to those described by the analysis of Craik,[34] and that when αR_L and α^2 are small, the relevant instability is a kinematic one.

The liquid-layer stability problem was also considered by Lane and Ruger wherein the surface boundary conditions for the sublimer in the analysis previously discussed were modified accordingly. Contrary to the result for the sublimer in which no conditions for instability were found, when the liquid layer was considered instability domains were obtained. Results for a 6.33° ablating Teflon cone are shown in Figs. 23 and 24 (l_l is the liquid-layer depth). This calculation was performed for a recovered flight vehicle under conditions corresponding to the altitude at which the maximum surface pressure occurred. The results for wave angle are in good agreement with those measured on the recovered vehicle (Fig. 23), whereas the non-dimensionalized pattern wavelengths are somewhat lower than observed (Fig. 24). In contrast to the 6.33° Teflon cone results, consideration of a 40° Teflon cone yielded wavelengths substantially in agreement with experiment, but pattern angles that were on the order of 50% too high.

An interesting aspect of the work of Lane and Ruger is worthy of note. Recall that Nachtsheim,[31] in his consideration of uniform flow over a thin liquid layer, found that the effects of surface tension were essential to achieving neutral stability from his analysis. Lane and Ruger, on the other hand, considering a boundary-layer flow over a thin liquid layer, found that surface tension played an insignificant role in determining the stability boundary. Thus, it appears that the simplified model of Nachtsheim may lead to spurious results regarding the role of surface tension in the over-all phenomenon.

As a check on the liquid-layer stability theory, Nachtsheim and Hagen[35] performed an experiment in which low-vapor-pressure, high-viscosity liquids were exuded near the tip of a 10° half-angle cone in a cold supersonic stream in an effort to determine if

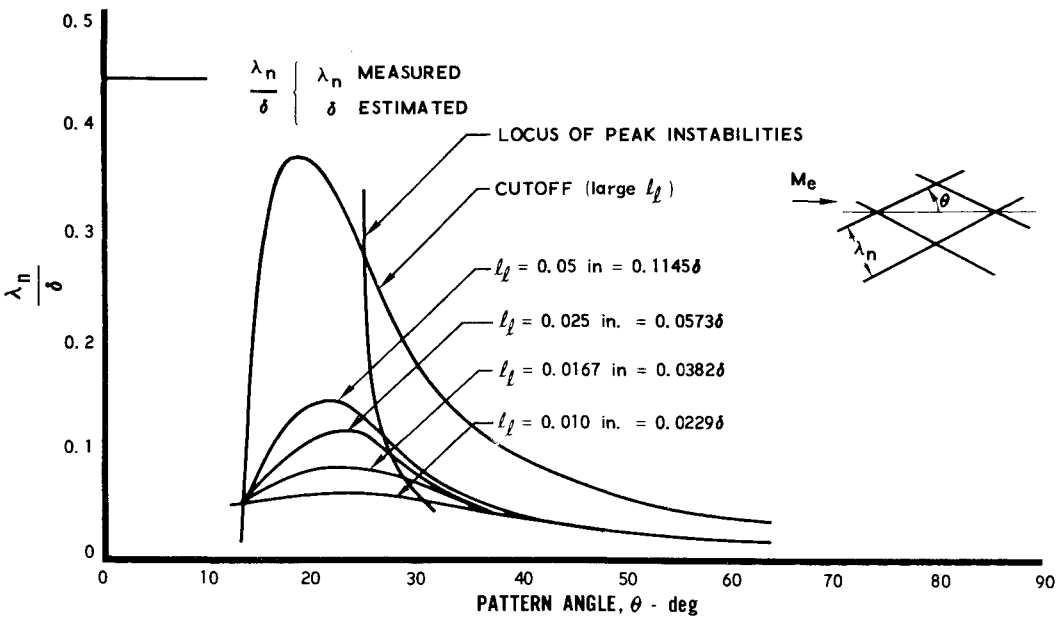

Fig. 24 Wavelength vs pattern angle based on analysis of Lane and compared with data.

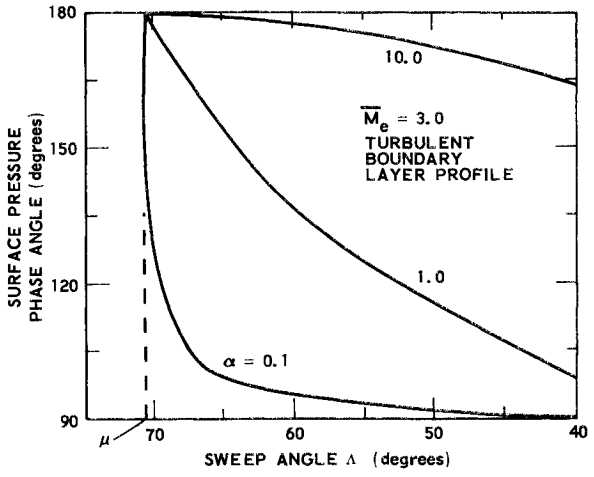

Fig. 25 Surface pressure phase-wave angle relationship for a turbulent boundary-layer Mach number profile as calculated by Gold, Probstein, and Scullen.[37]

differential sublimation or vaporization is a requirement for the formation of cross-hatched patterns. Cross-hatched patterns were observed during the tests, and it was concluded that ablation is not essential to the formation of cross-hatched surface patterns in supersonic flow. Moreover, the results were compared with the stability boundary corresponding to the test conditions as determined by Nachtsheim's analysis.[31] The test results fell in the predicted region of wave amplification.

In addition, a test was performed invoking the hydraulic analogy by flowing a supercritical layer of water over a porous conical model in which honey was exuded under pressure through the surface pores. The honey corresponds to a liquid film, and the supercritical water flow corresponds to inviscid supersonic flow by the hydraulic analogy. Cross-hatched patterns were observed to form, and it was concluded that the pattern arises from the viscous damping of the supersonic pressure disturbances by the liquid film, in accord with Nachtsheim's theory.

Thus, based on the work of Nachtsheim, Ko, Nayfeh and Saric, and Lane and Ruger, it may be concluded that liquid-layer instability is a physically realizable mechanism for the development of cross-hatched surface patterns.

D. Surface Deformation Mechanism

Probstein and Gold[36,37] postulated that cross hatching is the result of differential deformation due to relaxation and creep within the material, as opposed to differential ablation and liquid-layer instability. The governing equation for the boundary-layer flow was again taken to be Lighthill's equation for the perturbation pressure, containing wave number normal to the wave front and complex wave speed as parameters. Results of numerical integration through the boundary layer for various boundary-layer profiles having edge Mach numbers of three are shown in Figs. 25 and 26. In these calculations, the wave speed and amplification rate were taken equal to zero. Figure 25 shows the phase angle between the surface pressure and a sinusoidal wall as a function of the sweep angle for a turbulent boundary-layer profile and various values of the wave number α where $\alpha = 2\pi\delta/\lambda$, δ being the boundary-layer thickness, and λ the wavelength normal to the waves. In this formulation, a 90° phase shift corresponds to the pressure peaking at the point of maximum wall slope (as it does in the inviscid supersonic-flow solution), and a 180° phase shift corresponds to the pressure peaking at the trough of the wave (as it does in the inviscid subsonic-flow solution). Note that for small wave numbers, the boundary layer behaves as if it were uniform and supersonic except for sweep angles near the Mach angle. On the other hand, for large wave numbers the boundary layer exhibits subsonic behavior, indicating that a substantial phase shift is occurring across the subsonic portion of the boundary layer near the wall. Figure 26 shows the results for surface-pressure phasing for three representative boundary-layer Mach number profiles and a fixed small value of wave number. Note that the laminar profile exhibits a subsonic behavior, whereas the stepped profile behaves as if mainly supersonic. At the higher wave numbers, all profiles were noted to behave subsonically.

Probstein and Gold investigated the stability of a deformable surface under the abovementioned imposed flows by considering two simple mechanical deformable-surface models, namely those corresponding to the so-called Maxwell and Kelvin bodies. The idea of mechanical models is that combinations of basic elements are considered that are supposed to behave mechanically like constituent phases of the material, but which, apart from this mechanical behavior, have nothing in common with the real material. The mechanical models devised to illustrate inelastic behavior are usually built up of two elements, an elastic spring representing elastic deformation, and a dashpot representing viscous deformation. When these elements are coupled in series, a model of the Maxwell body is obtained. When the elements are coupled in parallel, a model of the Kelvin body is produced. The results of the stability investigation indicate the surface disturbance to be stable for the Kelvin body, but unstable for the Maxwell body when nonuniform boundary-layer Mach number profiles are considered. (For a uniform Mach number profile, instability is obtained for the Kelvin body.[36] This problem was also treated as an aeroviscoelastic problem by Dowell.[38]) The amplification rate for the Maxwell body was calculated as a function of wave number for the three different boundary-layer profiles mentioned previously. The results show that the turbulent profile results in the strongest amplification, but no wave number of peak amplification is indicated. Hence, the theory is unable to predict the most unstable disturbance wavelength. Moreover, for given wave number, the results indicate that the amplification rate increases monotonically with decreasing wave angle. Hence, the theory is unable to predict a preferred wave angle, either. However, it was estimated from the results that the most unstable wavelength λ is related to the properties of the material and the flow by

$$\lambda \sim \mu U_e/p_e M_e^2 c_f \tag{4}$$

where μ is the viscosity of the material, U_e, p_e, and M_e the edge velocity, pressure, and Mach number, respectively, and c_f the skin-friction coefficient. Thus, the only material property that disturbance wavelength depends upon is the viscosity. Note that, for turbulent boundary-layer flows with nearly constant edge conditions such as sharp-cone flows, the pattern wavelength is only weakly dependent on streamwise distance. This is in accord with experimental observation.

Lane[39] also considered the viscoelastic problem using a generalized Maxwell model to characterize the deformable

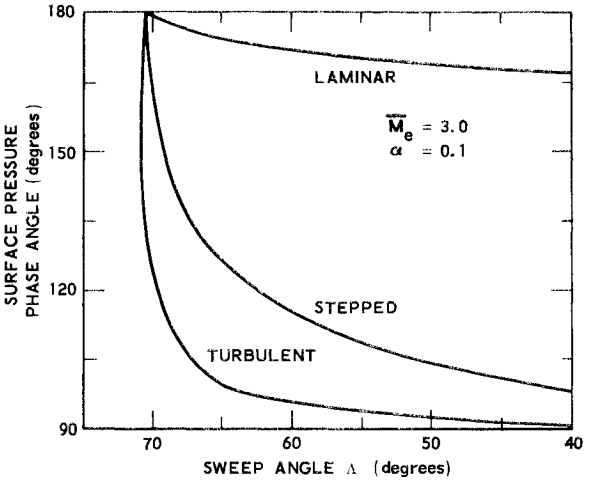

Fig. 26 Surface pressure phase angle-wave angle relationship for different boundary-layer Mach number profiles as calculated by Gold, Probstein, and Scullen.[37]

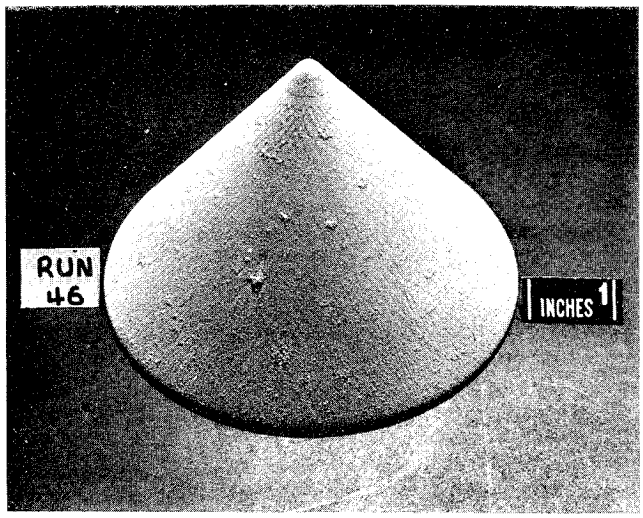

Fig. 27 Cross hatching on 40° Teflon (FEP) cone tested at NASA Ames.

surface. Under the assumption that the viscoelastic layer is incompressible, he showed that the viscoelastic case is equivalent to that for an incompressible liquid layer with a frequency-dependent viscosity when appropriate modifications in the material surface-gas flow boundary conditions are made. Moreover, he showed that the domain of instability of the viscoelastic layer in wave-number space is a subdomain of the domain of instability of the liquid layer which may, however, be nonexistent or empty. Although no numerical results were generated, certain conclusions were drawn based on the stability conditions of the analysis. First, he found that the relaxation time only entered the calculations in combination with the frequency, affecting pattern celerity and growth rate, but not wavelength. The parameters determining pattern existence, wavelength, and wave angle were found to be the effective spring constants (shear moduli) of the generalized Maxwell model and the relative amplitudes and phases of the perturbation pressures and shear stresses in the gas boundary layer. This is in contrast to the results of Probstein and Gold previously discussed.

Stock and Ginoux,[40] in an effort to check the validity of the surface-deformation theory, tested two 13° half-angle wax cones in a Mach 5.3 flow under the same stagnation conditions. The cones were of different initial ablation material temperature (290°K and 332°K), however, the higher temperature model having been preheated for 15 min at close to the liquefaction temperature of wax. Substantially larger patterns were observed to form on the preheated wax model. Effects of wall temperature were ruled out, since it was argued that both models would have the same surface temperature after a time short compared with the run time. Although the higher-temperature model had a larger mass-loss rate than the one at lower temperatures, this effect was deemed to be minor by Stock and Ginoux based on experiments in which cross-hatched patterns were noted to develop but very little ablation was observed. It was concluded by Stock and Ginoux that, since the viscosity and shear modulus of wax show considerable variations with temperature in the range 290–332°K, whereas boundary-layer properties and material density, specific heat, and thermal conductivity show little change in this temperature range, that ablation material viscosity and resistivity are important parameters in the formation of the cross-hatched pattern. Thus, Stock and Ginoux believe the results of this test lend support to the hypothesis of Probstein and Gold that cross hatching is the result of differential deformation of a viscous inelastic solid. Based on Eq. (4), however, it would appear that the preheated model should have smaller, rather than larger patterns, since the material viscosity would be lower.

A critical experiment to check out the surface deformation theory of Probstein and Gold was run by Nachtsheim at NASA Ames.[36] The model tested was a 40° half-angle Teflon (FEP) cone of 5-in. base diameter (Fig. 27). Probstein and Gold reported that the material properties were such that, under the test conditions and test time imposed, the model did not ablate (sublime or form a discernible liquid melt), and that post- and pretest weights were the same to within 0.1-g accuracy for the 650-g model, indicating no mass loss. The question of the presence of a liquid layer during this experiment is not a closed one, however, since a definite bead of Teflon was observed around the edges of the base after the test.[41] Hence, liquefaction of the surface material, subsequent flow down the cone, and resolidification on the base would also support the observed results.

Thus, based on the abovementioned results, the question of whether or not differential surface deformation in the absence of material ablation or surface melt is a viable physical mechanism for the development of cross-hatched surface patterns is still an open one. Additional critical experiments will be needed to fully answer this question.

IV. Additional Experimental Results

In addition to the experimental results discussed relative to various theories in the previous section, other experiments were performed that provided useful information. These experiments are discussed in this section.

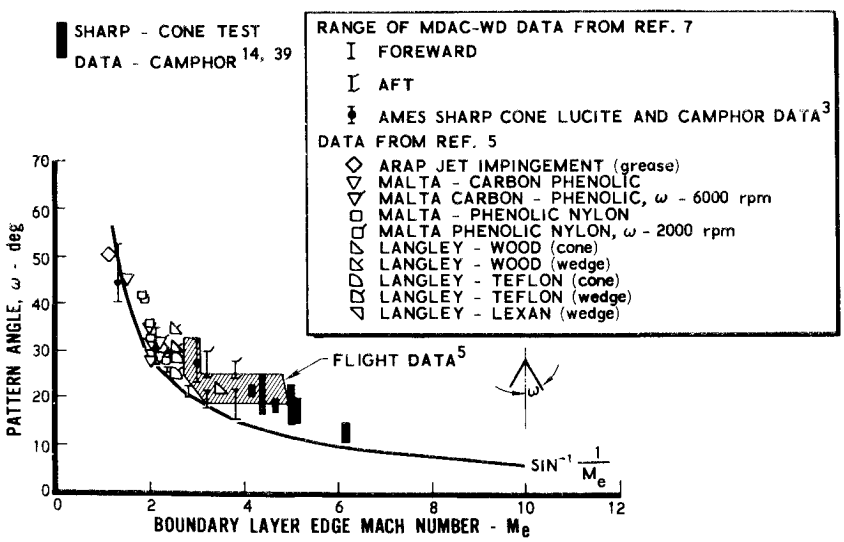

Fig. 28 Surface pattern angles as a function of local Mach number; from Williams and Inger.[42]

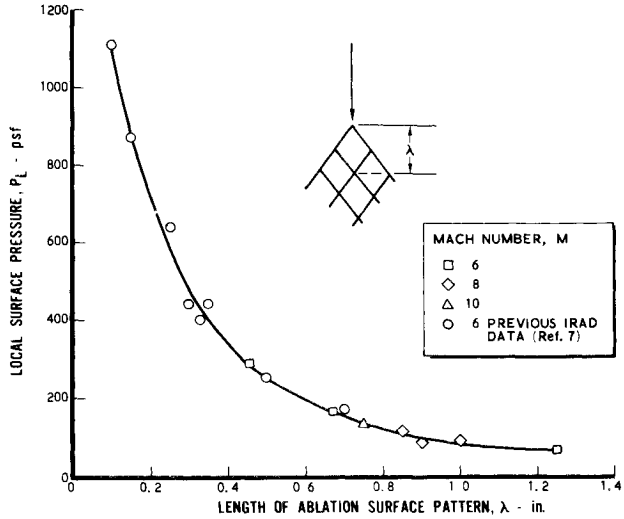

Fig. 29 Variation of camphor ablation surface pattern length with local surface pressure based on experiments of Williams and Inger.[7,16,42]

A. Williams and Inger

In addition to the wavy-wall experiments previously discussed, Williams and Inger[16,42] undertook another set of experiments involving the testing of 6°, 10°, and 16° steel-tipped camphor and Korotherm cones at freestream Mach numbers of 6, 8, and 10. Prior to these tests, pattern angle data were available for boundary-layer edge Mach numbers only up to about four and a plot of these quantities (Fig. 28) indicated a possible freezing out of pattern angle to a constant value for edge Mach numbers of about three and above. It was desired to obtain data for higher edge Mach numbers to investigate whether or not the freeze out was occurring. The results from the camphor cone tests are also shown in Fig. 28, indicating that the freeze out is not occurring.

To further investigate the freeze-out question, the effect of nose-tip blunting on cross hatching was investigated by testing a 10° cone with various radius nose tips.[42] The results show that the data, which were plotted at the correct local edge Mach number taking nose blunting into account, fit the sharp-cone correlation. If uncorrected, data for a bluntness ratio of 0.15 would violate the correlation and appear to be freezing out. Thus, when nose bluntness effects are taken into account, there is no indication of a limiting pattern angle above Mach 3 as suggested by the flight data of Fig. 28. Most likely sharp-cone calculations were used for the flight data, when in actuality significant nose blunting had occurred.

In addition, data were obtained by Williams,[7] and by Williams and Inger[16,42] to extend the previously noted correlation between pattern wavelength and surface pressure first suggested by Canning et al.[1] The result for camphor is shown in Fig. 29. It will be shown later (Sec. V) that the wavelength-pressure correlation is material-dependent, with similar correlations holding for other materials.

In an effort to determine the heat-transfer distribution, an epoxy casting was made from a post-test rubber mold of a 10° camphor cone previously tested at Mach 6. This casting material was selected since it would not ablate under the original test conditions. Radial segments of the model were covered with phase-change paint (Tempilaq), and the epoxy model retested at the original test conditions. The center segment was coated with 150°F Tempilaq and right and left segments with 225°F and 250°F Tempilaq, respectively. The 150°F paint melted on insertion of the model into the test stream. Color movies and 35-mm photographs show the 225°F and 250°F paints melting first in the pattern troughs, starting forward and moving aft on the body. Thus, the results of this test indicate higher heat-transfer rates in the troughs than at the crests.

B. Stock and Ginoux

Stock and Ginoux[14,40,43] investigated many aspects of cross hatching using wax and camphor cones in a Mach 5.3 flow. In Ref. 14, cones varying in total vertex angle from 10°–50° with pointed steel tips, and 10° cones with 12°–40° flares were tested. Results are shown in Figs. 30–32. Figure 30 shows results for the pattern angle as a function of edge Mach number in the edge Mach number range of 3–5. Note that the data follow the Mach-angle trend and show no tendency to freeze out, in agreement with the results of Williams and Inger previously discussed. Moreover, data for pattern wavelength vs edge pressure were obtained at lower edge pressures than considered by Williams and Inger (Fig. 31). Thus, the pattern wavelength-edge pressure correlation is extended. Note that both the wax and camphor

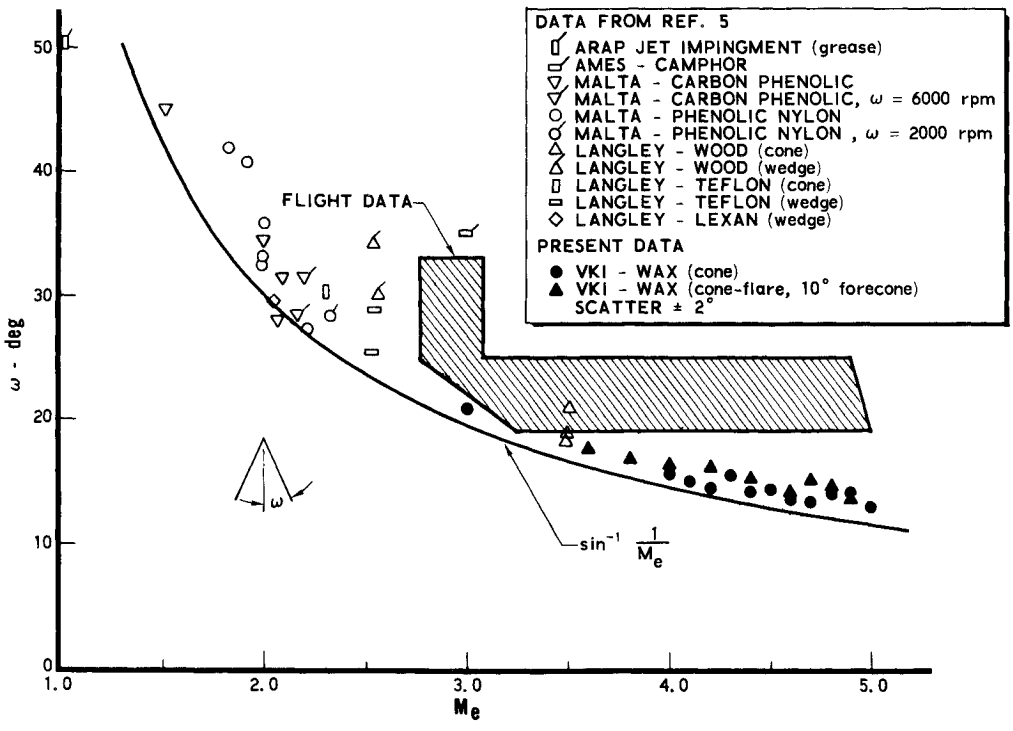

Fig. 30 Pattern angle vs edge Mach number, including wax-cone data of Stock and Ginoux.[40]

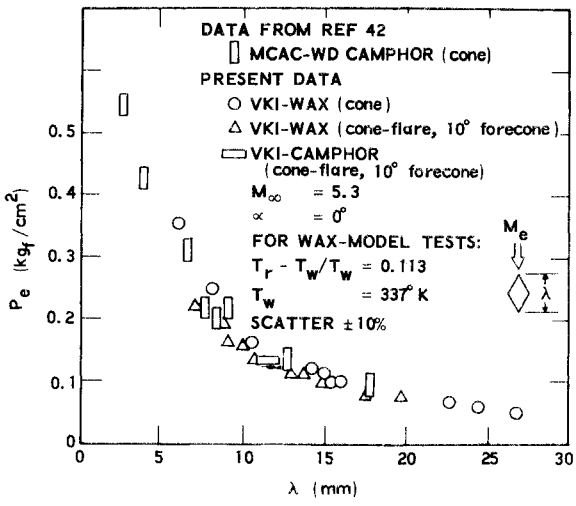

Fig. 31 Influence of local static pressure p_e on the streamwise spacing λ; based on the work of Stock and Ginoux.[40]

data fall on the same curve, indicating a similarity of response by these two materials.

In addition, the effect on pattern wavelength of driving temperature ratio $(T_r - T_w)/T_w$, where T_r is the recovery temperature and T_w the wall temperature, is shown in Fig. 32. Note that the streamwise wavelength increases nearly linearly with the temperature ratio. A similar result was noted by Canning et al[3]. for Plexiglas. This might also be interpreted as an ablation-rate effect. No indication of the relative ablation rates among the data are given, however.

Additional facets of the cross-hatching phenomenon were studied by Stock and Ginoux in Refs. 40 and 43. Self-blunting cones were tested in order to further investigate the possible relationship between blunting and the apparent freezing of pattern angle for flight data above edge Mach numbers of about three as discussed before. Results showed that the self-blunting data based on the calculated sharp-cone edge Mach numbers agree with the free-flight results, lending further support to the argument that the apparent freezing of the flight data is due to the erroneous use of edge Mach numbers calculated without taking nose blunting into consideration.

C. Nachtsheim and Larson

In an effort to obtain additional information regarding material property effects on the surface pattern, a series of tests was run by Nachtsheim and Larson[44] on Teflon and filled Teflon cones. The filler materials were graphite (15%) and borosilicate (7%, 15%, 20%, and 25%). The graphite-filled cones exhibited cross hatching, but the results for the glass-filled cones showed that as the percentage of glass was increased the pattern gradually disappeared, with the 25% glass-filled model displaying no pattern at all. The test results were interpreted in light of the previously discussed liquid-layer theory of Nachtsheim. Recalling the result for the neutral stability curves (Fig. 20), a sufficient increase in melt-layer Reynolds number should result in elimination of the pattern. In the abovementioned tests, a melt runoff was observed for glass-filled Teflon but not for the 100% Teflon model, the amount of runoff increasing with percentage of glass in the fill.

Aside from altering the viscosity of the melt layer, however, it might be argued that adding glass to TFE results in a less deformable material. To investigate whether it is the antideformation qualities of glass-filled TFE or the viscosity of the melt layer that governs pattern suppression, tests were run for both a 20% Refrasil-filled model and a 20% borosilicate-filled model. Refrasil is much more viscous than borosilicate, and hence should be more resistant to deformation. The results of the test are shown in Fig. 33. The Refrasil-filled model exhibited cross hatching and the borosilicate-filled model did not. The results of this test were interpreted as indicating that the pattern is influenced more by the viscosity of the melt layer than by its antideformation properties.

In addition to the filled Teflon models discussed proviously, Nachtsheim and Larson also tested fiberglass-phenolic and quartz-phenolic cones in the Marshall Space Flight Center rocket motor facility. The fiberglass-phenolic model was characterized by substantial material loss and a relatively coarse cross-hatched pattern, in contrast to the low ablative mass loss and fine pattern of the quartz-phenolic model. Thus, it is again evident that material properties play a significant role in determining cross-hatched pattern characteristics.

D. Lees, Kubota, and Sigal

A low-speed (freestream velocity 50 fps) experiment was undertaken by Lees, Kubota, and Sigal[45] to study the interaction between a turbulent boundary layer and a wavy wall. Two wavy-wall models with ratio of amplitude to wavelength of 0.03 and wavelengths of 6 and 12 in. were tested. Boundary-layer thicknesses varied from 1.5 in. to 4 in. giving a wavelength

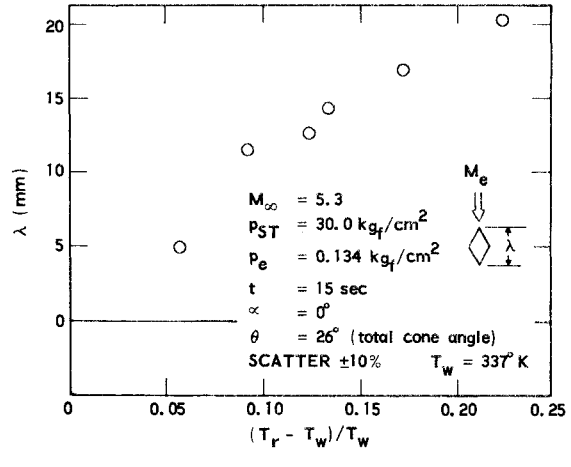

Fig. 32 Influence of the driving temperature ratio $(T_r - T_w)/T_w$ on the streamwise spacing λ based on the work of Stock and Ginoux.[40]

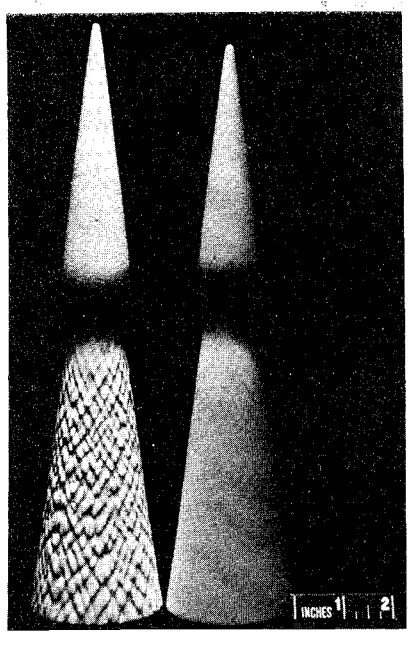

Fig. 33 Results of testing filled Teflon cones. Refrasil-filled TFE on left, borosilicate on right; from Nachtsheim and Larson.[44]

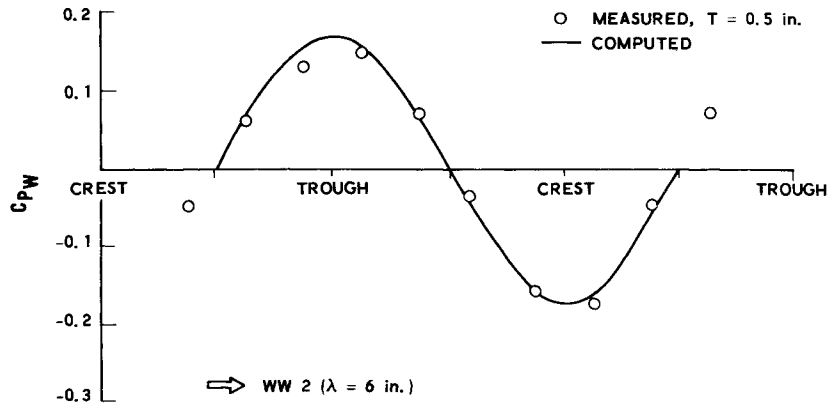

Fig. 34 Comparison between computed and measured wall pressure distribution—experiments of Lees, Kubota, and Sigal.[45]

to boundary-layer thickness-ratio range of 1.5–8. One of the objectives of the tests was to check the validity under the presence of curvature effects of turbulence models that relate turbulent stresses either to mean-flow quantities or to turbulent energy. Since it is easier and less expensive to make detailed measurement in a low speed as opposed to a high-speed flow, if results from the analytical model showed good agreement with experiment in the low-speed case then this would lend confidence in use of the model for the high-speed case. Typical results from the experiment for surface pressure distribution, wall shear, and Reynolds stress, and comparison with a theoretical calculation employing the effective eddy-viscosity model of Cebeci et al.[46] are shown in Figs. 34–36. Recall that the uniform subsonic flow solution predicts the pressure peaking in the troughs; Fig. 34 shows it to be peaking about 10°–15° behind the trough. Whereas good agreement between theory and experiment is obtained for the pressure distribution, only fair agreement is achieved for wall shear and Reynolds stress. Results were also compared with two other models for shear stress and it was determined that, because of rapid changes in stress distribution near the wall and the modulation of mixing length and eddy viscosity in the outer layer, none of these models was adequate for the wavy-wall pattern. It was found, however, that if mixing length and eddy viscosity are based on the total velocity, defined as

$$U^t = \{\bar{U}^2 + [2(p - p_o)/\rho]\}^{1/2}$$

where $\bar{U}$ is the mean velocity, p the pressure, p_o a reference pressure, and ρ the density, then the distribution of mixing length and eddy viscosity for all stations over a wavy wall is identical to the corresponding curves for a flat plate boundary layer. No turbulent boundary-layer calculations using these revised definitions for mixing length and eddy viscosity were carried out, however.

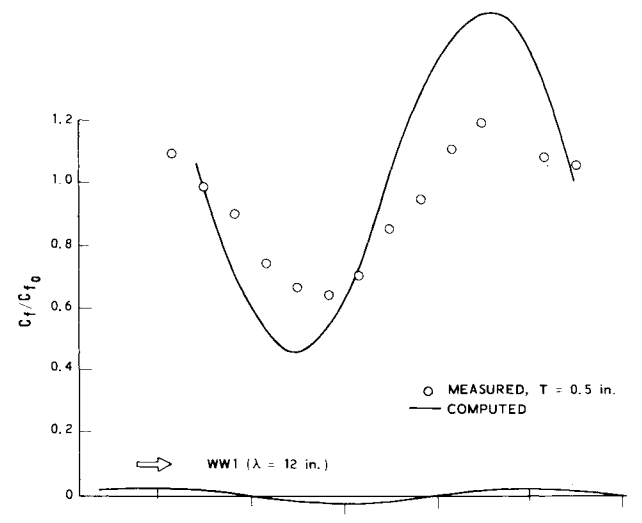

Fig. 35 Comparison between computed and measured wall shear distribution—experiments of Lees, Kubota, and Sigal.[45]

V. Correlation Studies

In a further effort to define the most probable physical mechanism or mechanisms governing cross-hatch pattern for motion under a given set of conditions, data correlation studies based on parameters generated by theory were undertaken by White and Grabow of Philco-Ford Corp.[23,24] These investigators evaluated the amplification-rate equations for differential ablation (Inger), surface deformation (Probstein and Gold), and surface-flow theories,[24] and determined the wave angles corresponding to the maximum-amplification condition for each theory. The surface-flow theory combines the inviscid solution of Conrad and Donaldson[22] and the viscous sublayer result of Inger[18,19] with the dispersion relation of Craik[33] for the low-speed stability of a thin liquid film. There results,[23] for high viscosity surface flows under supersonic conditions

$$\overline{\alpha c_i} = 18.4\left(\frac{\delta_L}{\lambda_L}\right)^3 \frac{p_e}{\mu_L}\frac{\hat{p}_{\text{mag}}\cos\Phi_p}{\delta/\lambda_L}\left[1 + \frac{1.1\mu_w^{2/3}\lambda_L^{1/3}}{\delta_L(\rho_w\tau_w)^{1/3}} \times \frac{\sin(\Phi_p + 120)}{\cos\Phi_p}\right] \quad (5)$$

where αc_i is the amplification rate, δ_L, λ_L, and μ_L are the surface layer thickness, pattern longitudinal wavelength, and surface-layer viscosity, respectively, p_e is the boundary-layer edge pressure, $\hat{p}_{\text{mag}}$ the pressure perturbation amplitude, ϕ_p the phase angle between the pressure and the wall (taken as zero in the valleys), δ the boundary-layer thickness, and μ_w, ρ_w, τ_w the wall values of viscosity, density, and shear stress, respectively.

Equation (5) is used for the prediction of wave angle and neutral stability, the wave angle being that corresponding to conditions of maximum amplification, and the neutral-stability condition corresponding to zero amplification. It is stated[24] that the maximum amplification condition corresponds to $\hat{p}_{\text{mag}}\cos\phi_p$ being a maximum. In general, however, ϕ_p is not independent of wave angle[22] and boundary-layer thickness to wavelength ratio, and Eq. (5) yields the result that the amplification rate is proportional to the sum of two terms, the first involving $\hat{p}_{\text{mag}}\cos\phi_p$ and the second $\hat{p}_{\text{mag}}\sin(\phi_p + 120)$. This correction may affect the results shown in Figs. 17a and 17b.

In general, all three theories show that the maximum-amplification condition is primarily a function of the inviscid pressure perturbation field and the phase lag of the heat-transfer or shear perturbations. To make a consistent comparison of the results, the same inviscid pressure perturbation field was used, namely that of Conrad, Donaldson, and Snedeker[22] previously discussed. Again consider Fig. 17a. Shown thereon are wave-angle correlations for Teflon, including comparisons with the three theories. The differences between the results shown are

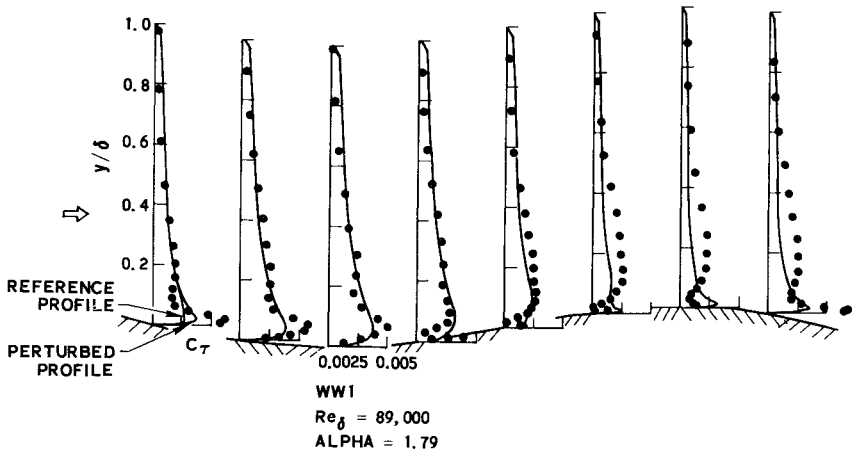

Fig. 36 Comparison between computed and measured Reynolds stress profiles—experiments of Lees, Kubota, and Sigal.[45]

strictly due to the differences in phase lag between the heat-transfer or shear and pressure perturbations, being zero (as assumed by Conrad, Donaldson, and Snedeker) for the surface flow result, 42° for the differential ablation result, and 60° for the surface deformation result. A similar wave-angle correlation for other materials is shown in Fig. 17b.

An expression for the stability boundary is obtained by setting Eq. (5) equal to zero. Under the assumption that $\phi_p = 75°$ there results[23]

$$\lambda_N \sim \delta_L{}^3 p_e \tau_{wN}/T_w{}^{2.2} \tag{6}$$

where λ_N is the pattern wavelength normal to the grooves, δ_L the liquid-layer thickness, p_e the boundary-layer edge pressure, and τ_{wN} and T_w the wall shear in the normal direction, and wall temperatures, respectively. As previously indicated, however, ϕ_p is not independent of pattern wave angle and wave number. This is shown in Fig. 25 taken from Ref. 37, which shows the results of integrating the inviscid Lighthill equation for the perturbation pressure through a turbulent boundary layer. The surface pressure phase angle shown is equal to (180-ϕ_p) deg (also, sweep angle $\Lambda = 90\text{-}\omega°$ and $\alpha = 2\pi\delta/\lambda_N$). Thus, for a given wave angle a wavelength-surface pressure phase angle relationship is implied.

Attempts at data correlation using Eq. (6) were not fruitful, however. Grabow and White then assume, based on the results of Refs. 24 and 31, that $\lambda_N \sim \delta_L$ which, combined with Eq. (6), yields

$$\lambda_N \sim T_w{}^{1.1}/(p_e \tau_{wN})^{1/2} \tag{7}$$

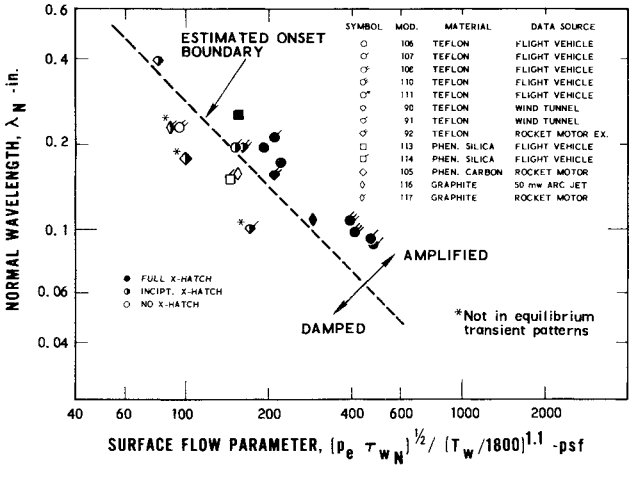

Fig. 37 Cross-hatching stability boundary—comparison of theoretical prediction of White and Grabow[23,24] with data for high-temperature ablators.

Comparison of this predicted correlation shows good agreement with data for high-temperature ablators (Fig. 37). This appears fortuitous, however, as the results of Ref. 24 show $\lambda_N/\delta_L \sim (\delta_L/\delta)^{0.6}$, where δ is the boundary-layer thickness, and Ref. 31 shows λ_N/δ_L to be a function of the interaction parameter previously discussed.

In addition, the previously mentioned pattern wavelength-surface pressure correlation uncovered by Williams and Inger for camphor (Fig. 29) was extended by White and Grabow[24] to other materials (Fig. 38). Again, under the assumption that $\lambda_L \sim \delta_L$, a physical basis for this correlation is developed for material in a steady-state high ablation mode in which the liquid or deformable layer thickness is inversely proportional to the recession rate. Hence, it is argued[24] that this correlation does not hold for melting ablators under transient thermal response conditions.

Based on the abovementioned data correlation studies, White and Grabow concluded that the liquid-layer mechanism is the most likely to be occurring. As indicated, however, many assumptions are involved in arriving at this conclusion. Hence, these correlation studies should not be considered absolutely conclusive.

VI. Discussion

Several physical mechanisms that may govern the development of cross-hatched surface patterns in ablative or deformable materials have been investigated. Theories based on the presence of longitudinal vorticity or wall cooling in order to achieve conditions conducive to pattern development have been set forth. Others relying on heat conduction, liquid-layer surface tension, or particular response characteristics of a deformable surface have been developed. Moreover, experimental results have been obtained that verify the pressure and heat-transfer distributions predicted by certain theories for a nearly stationary amplifying pattern. Additional experimental results indicate material property modifications needed to suppress or eliminate the pattern, and the probable physical mechanism governing the pattern when a liquid layer is present. Other experiments have indicated that longitudinal vortices are not essential to pattern initiation and development, while still others have been performed to verify or disprove the anelastic deformation theory. These theories and experimental results will now be discussed in light of differing conclusions in the case of the theories, and differing interpretations in the case of the experiments.

For a subliming ablator, the detailed numerical results of Lees and Kubota[26] indicated instability domains for certain wavelengths and wave angles. Comparable results of Lane and Ruger indicate that no instability occurs for the sublimer. As brought out by the experimental work of Lees, Kubota and Sigal,[45] however, the turbulence models used in these calculations are not adequate for the wavy-wall problem. As a result, firm conclusions cannot be drawn from them. Other work, notably that of

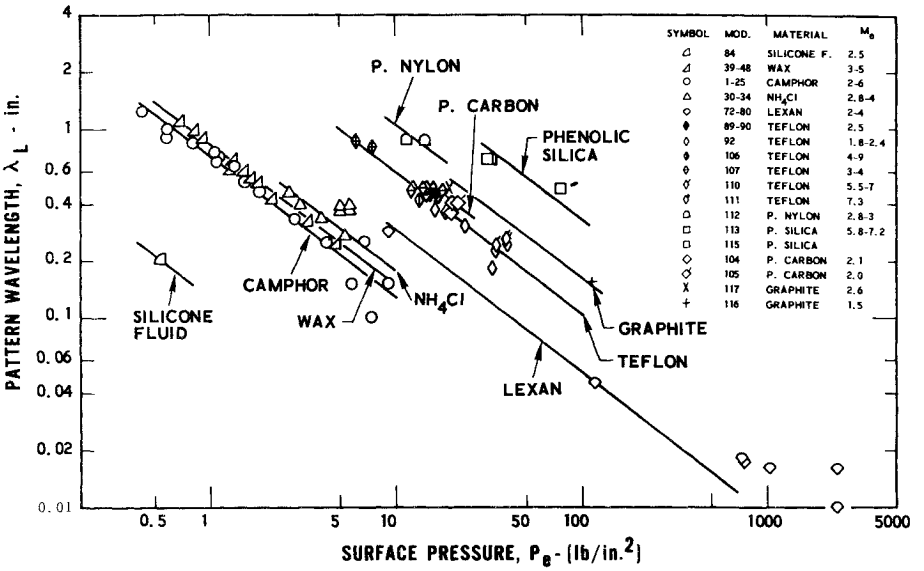

Fig. 38 Pattern wavelength—surface pressure correlation based on work of White and Grabow.[23,24]

Williams,[7] Inger,[18,19] and Williams and Inger[16,17] lends support to the sublimation mechanism.

For the liquid layer, finite surface tension was essential in obtaining a stability boundary in the analysis of Nachtsheim.[31] Recall that Nachtsheim postulated a uniform gas flow adjacent to the liquid layer, however. When the same problem was examined by Lane and Ruger employing a numerical turbulent boundary-layer solution for the outer flow, the role of surface tension was found to be negligible. Hence, it appears that the spurious role of surface tension in Nachtsheim's analysis may be the result of the uniform outer gas flow assumption.

Turning now to interpretation of experiment, Probstein and Gold[36] reported on the results of a Teflon cone tested at NASA Ames whereby cross hatching was observed but no weight loss indicated. They contended that the result lent support to the inelastic deformation theory. Nachtsheim,[41] on the other hand, reported that post-test examination revealed beads of material on the base of the cone, indicating that perhaps a liquid layer had formed. In a further effort to clarify the surface deformation-liquid layer question, Nachtsheim and Larson[44] ran a test whereby two Teflon cones, one 20% filled with a low-viscosity glass (borosilicate) and the other filled with an identical percentage of high-viscosity glass (Refrasil), were tested under identical conditions. The cone containing the Refrasil exhibited cross hatching, whereas the borosilicate-filled cone did not. The Refrasil-filled cone, having the higher viscosity, should exhibit better antideformation properties than the borosilicate cone. On the basis of this test, Nachtsheim and Larson concluded that it is the melt-layer viscosity rather than the room-temperature antideformation qualities of glass-filled Teflon that matters insofar as the formation of a cross-hatched pattern is concerned.

Finally, with regard to data-correlation studies, White and Grabow concluded that the surface-flow mechanism is most likely governing the development of cross-hatched patterns. This result, however, is based on a number of assumptions, and thus cannot be considered conclusive.

VI. Conclusions

As a result of the studies discussed herein, the following major conclusions are drawn.

a) For the case of the subliming ablator, experimental evidence and certain theoretical analyses support pattern formation by differential ablation, whereas other theoretical studies indicate that patterns should not form in such materials by this mechanism. Hence, definitive theoretical and/or experimental work is still needed to resolve the question of pattern formulation by differential ablation.

b) Theoretical and experimental bases have been established for the formation of cross-hatched surface patterns in melting ablators, and a theoretical basis has been established for their formation in anelastic deformable materials. A definitive critical experiment is still needed for verification of the anelastic deformation mechanism, however.

c) The presence of longitudinal vortices is not a necessary requirement for the initiation and development of cross-hatched surface patterns.

d) Conditions for pattern onset are predictable for a wide range of materials.

e) Pattern wave angles and wavelengths are predictable for a wide range of materials.

f) Ways of altering material properties to suppress cross hatching have been indicated.

References

[1] Canning, T. N., Wilkins, M. E., and Tauber, M. E., "Boundary-Layer Phenomena Observed on the Ablated Surfaces of Cones Recovered after Flight at Speeds up to 7 km/sec," AGARD Proceedings No. 19, May 1967.

[2] Canning, T. N., Wilkins, M. E., and Tauber, M. E., "Ablation Patterns on Cones having Laminar and Turbulent Flows," *AIAA Journal*, Vol. 6, No. 1, Jan. 1968, pp. 174–177.

[3] Larson, H. K. and Mateer, G. G., "Cross Hatching—A Coupling of Gas Dynamics with the Ablation Process," AIAA Paper 68-670, Los Angeles, Calif., 1968.

[4] Canning, T. N. et al., "Orderly Three-Dimensional Processes in Turbulent Boundary Layers on Ablating Bodies," *Hypersonic Boundary Layers and Flow Fields*, AGARD Proceedings No. 30, Paper No. 6, May 1968.

[5] Laganelli, A. L. and Nestler, D. E., "Surface Ablation Patterns: A Phenomenology Study," *AIAA Journal*, Vol. 7, No. 7, July 1969, pp. 1319–1325.

[6] Laganelli, A. L. and Zempel, R. E., "Observation of Surface Ablation Patterns in Subliming Materials," *AIAA Journal*, Vol. 8, No. 9, Sept. 1970, pp. 1709–1711.

[7] Williams, E. P., "Experimental Studies of Ablation Surface Patterns and Resulting Roll Torques," *AIAA Journal*, Vol. 9, No. 7, July 1971, pp. 1315–1321.

[8] Lipfert, F. and Genovese, J., "An Experimental Study of the Boundary Layers on Low-Temperature Subliming Ablators," *AIAA Journal*, Vol. 9, No. 7, July 1971, pp. 1330–1337.

[9] McDevitt, J. B., "An Exploratory Study of the Roll Behavior of Ablating Cones," *Journal of Spacecraft and Rockets*, Vol. 8, No. 2, Feb. 1971, pp. 161–169.

[10] Mirels, H., "Origin of Striations in Ablative Materials," *AIAA Journal*, Vol. 7, No. 9, Sept. 1969, pp. 1813–1814.

[11] Persen, L. N., "Surface Patterns of Ablating Bodies Studied by

means of Water Experiment Simulation," *Zietschrift für Flugwissenschaften,* Vol. 19, Aug.–Sept. 1971, pp. 360–373.

[12] Tobak, M., "Hypothesis for the Origin of Cross Hatching," *AIAA Journal,* Vol. 8, No. 2, Feb. 1970, pp. 330–334.

[13] Persen, L. N., "Streamwise Directed Vortices and Crosshatched Surfaces of Re-Entry Vehicles," *Journal of Spacecraft and Rockets,* Vol. 7, No. 1, Jan. 1970, pp. 108–110.

[14] Stock, H. W. and Ginoux, J. J., "Hypersonic Low Temperature Ablation—An Experimental Study of Cross-Hatched Surface Patterns," TN 64, July 1971, von Kármán Institute for Fluid Dynamics, Rhode-Saint-Genèse, Belgium.

[15] Inger, G. R., "Discontinuous Supersonic Flow past an Ablating Wavy Wall," *AIAA Journal,* Vol. 7, No. 4, April 1969, pp. 763–764.

[16] Williams, E. P. and Inger, G. R., "Investigation of Ablation Surface Cross Hatching," SAMSO TR 70-246, June 1970, McDonnell-Douglas Astronautics Co.—West, Huntington Beach, Calif.

[17] Inger, G. R. and Williams, E. P., "Subsonic and Supersonic Boundary-Layer Flow past a Wavy Wall," *AIAA Journal,* Vol. 10, No. 5, May 1972, pp. 636–642.

[18] Inger, G. R., "Compressible Boundary Layer Flow past a Swept Wavy Wall with Heat Transfer and Ablation," TN 67, Dec. 1970, von Kármán Institute for Fluid Dynamics, Rhode-Saint-Genèse, Belgium

[19] Inger, G. R., "Three-Dimensional Heat Transfer and Ablation Disturbances in High-Speed Flows," *AIAA Journal,* Vol. 10, No. 12, Dec. 1972, pp. 1641–1646.

[20] Lighthill, M. J., "Reflection at a Laminar Boundary Layer of a Weak Steady Disturbance to a Supersonic Stream, Neglecting Viscosity and Heat Conduction," *Quarterly Journal of Mechanics and Applied Mathematics,* Vol. 3, Pt. 3, 1950, pp. 302–325.

[21] Lighthill, M. J., "On Boundary Layers and Upstream Influence II. Supersonic Flows Without Separation," *Proceedings of the Royal Society,* Ser. A, Vol. 217, 1953, pp. 478–507.

[22] Conrad, P., Donaldson, C. duP., and Snedeker, R., "A Study of the Modal Response Approach to Patterned Ablation Including Experiment Definition," SAMSO TR 70-213 (ARAP Rept. 144), April 1970, Aeronautical Research Associates of Princeton, Inc., Princeton, N.J.

[23] Grabow, R. M. and White, C. O., "A Surface Flow Approach for Predicting Crosshatch Patterns," *AIAA Journal,* Vol. 11, No. 6, June 1973, pp. 841–847.

[24] White, C. O. and Grabow, R. M., "Crosshatch Surface Patterns—Comparison of Experiment with Theory," *AIAA Journal,* Vol. 11, No. 9, Sept. 1973, pp. 1316–1322.

[25] Lew, H. and Li, H., "The Analysis of the Transmission of Pressure Disturbances in the Formation of Surface Patterns," Sec. 7, RVTO Roll Phenomenology Final Report, Document 68SD809, July 1968, General Electric Co., Philadelphia, Pa.

[26] Lees, L., Kubota, T., and Ko, D. R.-S., "Stability Theory for Cross Hatching, Part I, Linear Stability Theory," SAMSO TR 72-34, Vol. I, Feb. 1972, California Institute of Technology, Pasadena, Calif.

[27] Sternberg, J., "A Theory for the Viscous Sublayer of a Turbulent Flow," *Journal of Fluid Mechanics,* Vol. 13, Pt. 2, June 1962, pp. 241–271.

[28] Sternberg, J., "The Three-Dimensional Structure of the Viscous Sublayer," AGARDograph 97, 1965.

[29] Schubert, G. and Corcos, G. M., "The Dynamics of Turbulence Near a Wall According to a Linear Model," *Journal of Fluid Mechanics,* Vol. 29, Pt. 1, July 1967, pp. 113–136.

[30] Klebanoff, P. S., "Characteristics of Turbulence in a Boundary Layer with Zero Pressure Gradient," TN 3178, 1954, NACA.

[31] Nachtsheim, P. R., "Stability of Crosshatched Wave Patterns in Thin Liquid Films Adjacent to Supersonic Streams," *The Physics of Fluids,* Vol. 13, No. 10, Oct. 1970, pp. 2432–2447.

[32] Nayfeh, A. H. and Saric, W. S., "Stability of a Liquid Film," *AIAA Journal,* Vol. 9, No. 4, April 1971, pp. 750–752.

[33] Craik, A. D. D., "Comments on 'Stability of Cross-Hatched Wave Patterns in Thin Liquid Films Adjacent to Supersonic Streams,'" *The Physics of Fluids,* Vol. 15, No. 5, May 1972, pp. 948–949.

[34] Craik, A. D. D., "Wind-Generated Waves in Thin Liquid Films," *Journal of Fluid Mechanics,* Vol. 26, Pt. 2, 1966, pp. 369–392.

[35] Nachtsheim, P. R. and Hagen, J. R., "Observations of Cross-hatched Wave Patterns in Liquid Films," *AIAA Journal,* Vol. 10, No. 12, Dec. 1972, pp. 1637–1640.

[36] Probstein, R. F. and Gold, H., "Cross-Hatching: A Material Response Phenomena," *AIAA Journal,* Vol. 8, No. 2, Feb. 1970, pp. 364–366.

[37] Gold, H., Probstein, R. F., and Scullen, R. D., "Inelastic Deformation and Cross-Hatching," *AIAA Journal,* Vol. 9, No. 10, Oct. 1971, pp. 1904–1910.

[38] Dowell, E. H., "Cross Hatching as an Aeroviscoelastic Problem," *AIAA Journal,* Vol. 10, No. 5, May 1972, pp. 701–703.

[39] Lane, F., "Viscoelastic-Material Version of the Self-Excitation Analysis for Striations of Ablating or Deforming Materials in Supersonic Flows with Turbulent Boundary Layers," TR 1, July 1971, KLD Associates, Huntington, N.Y.

[40] Stock, H. W. and Ginoux, J. J., "Further Experimental Studies of Cross Hatching," *AIAA Journal,* Vol. 10, No. 4, April 1972, pp. 557–558.

[41] Nachtsheim, P. R., private communication, June 1971, Mountain View, Calif.

[42] Williams, E. P. and Inger, G. R., "Ablation Surface Cross Hatching on Cones in Hypersonic Flow," *AIAA Journal,* Vol. 9, No. 10, Oct. 1971, pp. 2077–2078.

[43] Stock, H. W. and Ginoux, J. J., "Experimental Results on Cross-Hatched Ablation Patterns," *AIAA Journal,* Vol. 9, No. 5, May 1971, pp. 971–973.

[44] Nachtsheim, P. R. and Larson, H. K., "Cross-Hatched Ablation Patterns in Teflon," *AIAA Journal,* Vol. 9, No. 8, Aug. 1971, pp. 1609–1614.

[45] Lees, L., Kubota, T., and Sigal, A., "Stability Theory for Cross Hatching, Part II. An Experiment on Turbulent Boundary Layer Over a Wavy Wall," SAMSO TR 72-34, Vol. II, Feb. 1972, California Institute of Technology, Pasadena, Calif.

[46] Cebeci, T., Smith, A. M. O., and Mosinskis, G., "Calculation of Compressible Adiabatic Turbulent Boundary Layers," *AIAA Journal,* Vol. 8, No. 11, Nov. 1970, pp. 1974–1982.